17

PNL-5000 PT3
UC-11

Pacific Northwest Laboratory Annual Report for 1983 to the DOE Office of Energy Research

Part 3 Atmospheric Sciences February 1984

Prepared for the U.S. Department of Energy
under Contract DE-AC06-76RLO 1830

Pacific Northwest Laboratory
Operated for the U.S. Department of Energy
by Battelle Memorial Institute

Battelle

PACIFIC NORTHWEST LABORATORY
operated by
BATTELLE
for the
UNITED STATES DEPARTMENT OF ENERGY
under Contract DE-AC06-76RLO 1830

Printed in the United States of America
Available from
National Technical Information Service
United States Department of Commerce
5285 Port Royal Road
Springfield, Virginia 22161

NTIS Price Codes
Microfiche A01

Printed Copy

Pages	Price Codes
001-025	A02
026-050	A03
051-075	A04
076-100	A05
101-125	A06
126-150	A07
151-175	A08
176-200	A09
201-225	A010
226-250	A011
251-275	A012
276-300	A013

PNL-5000 PT3
UC-11

Pacific Northwest Laboratory Annual Report for 1983 to the DOE Office of Energy Research

Part 3 Atmospheric Sciences

C. E. Elderkin and Staff Members
of Pacific Northwest Laboratory

February 1984

Prepared for
the U.S. Department of Energy
under Contract DE-AC06-76RLO 1830

Pacific Northwest Laboratory
Richland, Washington 99352

PREFACE

This 1983 annual report from Pacific Northwest Laboratory (PNL) to the Department of Energy (DOE) describes research in environment, health, and safety conducted during fiscal year 1983. The report again consists of five parts, each in a separate volume.

The five parts of the report are oriented to particular segments of our program. Parts 1 to 4 report on research performed for the DOE Office of Health and Environmental Research in the Office of Energy Research. Part 5 reports progress on all research performed for the Assistant Secretary for Environmental Protection, Safety and Emergency Preparedness. In some instances, the volumes report on research funded by other DOE components or by other governmental entities under interagency agreements. Each part consists of project reports authored by scientists from several PNL research departments, reflecting the multidisciplinary nature of the research effort.

The parts of the 1983 Annual Report are:

Part 1: Biomedical Sciences Program Manager - J. F. Park	D. L. Felton, Report Coordinator and Editor
Part 2: Ecological Sciences Program Manager - B. E. Vaughan	B. E. Vaughan, Report Coordinator C. M. Novich, Editor
Part 3: Atmospheric Sciences Program Manager - C. E. Elderkin	N. S. Laulainen, Report Coordinator J. L. Downs-Berg, Editor
Part 4: Physical Sciences Program Manager - J. M. Nielsen	R. M. Garcia, Report Coordinator J. E. Danko, Editor
Part 5: Overview and Assessment Program Managers - S. Marks W. A. Glass	R. W. Baalman, Report Coordinator and Editor

Activities of the scientists whose work is described in this annual report are broader in scope than the articles indicate. PNL staff have responded to numerous requests from DOE during the year for planning, for service on various task groups, and for special assistance.

Credit for this annual report goes to many scientists who performed the research and wrote the individual project reports, to the program managers who directed the research and coordinated the technical progress reports, to the editors who edited the individual project reports and assembled the five parts, and to Ray Baalman editor in chief, who directed the total effort.

W. J. Bair, Manager
S. Marks, Associate Manager
Environment, Health and Safety Research
Program

Previous reports in this series:

Annual Report for

1951	W-25021, HW-25709
1952	HW-27814, HW-28636
1953	HW-30437, HW-30464
1954	HW-30306, HW-33128, HW-35905, HW-35917
1955	HW-39558, HW-41315, HW-41500
1956	HW-47500
1957	HW-53500
1958	HW-59500
1959	HW-63824, HW-65500
1960	HW-69500, HW-70050
1961	HW-72500, HW-73337
1962	HW-76000, HW-77609
1963	HW-80500, HW-81746
1964	BNWL-122
1965	BNWL-280; BNWL-235, Vol. 1-4; BNWL-361
1966	BNWL-480, Vol. 1; BNWL-481, Vol. 2, Pt. 1-4
1967	BNWL-714, Vol. 1; BNWL-715, Vol. 2, Pt. 1-4
1968	BNWL-1050, Vol. 1, Pt. 1-2; BNWL-1051, Vol. 2, Pt. 1-3
1969	BNWL-1306, Vol. 1, Pt. 1-2; BNWL-1307, Vol. 2, Pt. 1-3
1970	BNWL-1550, Vol. 1, Pt. 1-2; BNWL-1551, Vol. 2, Pt. 1-2
1971	BNWL-1650, Vol. 1, Pt. 1-2; BNWL-1651, Vol. 2, Pt. 1-2
1972	BNWL-1750, Vol. 1, Pt. 1-2; BNWL-1751, Vol. 2, Pt. 1-2
1973	BNWL-1850, Pt. 1-4
1974	BNWL-1950, Pt. 1-4
1975	BNWL-2000, Pt. 1-4
1976	BNWL-2100, Pt. 1-5
1977	PNL-2500, Pt. 1-5
1978	PNL-2850, Pt. 1-5
1979	PNL-3300, Pt. 1-5
1980	PNL-3700, Pt. 1-5
1981	PNL-4100, Pt. 1-5
1982	PNL-4600, Pt. 1-5

FOREWORD

The goals of atmospheric research at Pacific Northwest Laboratory (PNL) are to assess, describe and predict the nature and fate of atmospheric contaminants and to study the impacts of contaminants on local, regional and global climates. The contaminants being investigated are those resulting from the development and use of conventional energy resources (coal, gas, oil, and nuclear power) as well as alternative energy resources.

The description of atmospheric research at PNL is organized in terms of generic studies:

- Contaminant Characterizations and Transformation
- Boundary Layer Meteorology
- Dispersion, Deposition and Resuspension of Atmospheric Contaminants

Contaminant Characterization and Transformation

As assessment of the nature and fate of atmospheric contaminants must begin with a description of the chemical and physical nature of the materials being emitted from the source. Because many atmospheric contaminants are changed to other physical states and/or chemical forms, understanding these transformations is essential in any assessment. Of particular concern are those atmospheric transformations that produce potentially environmentally harmful or hazardous substances, such as strong acids, and mutagenic and carcinogenic compounds.

Boundary Layer Meteorology in Complex Terrain

Air pollution in mountaious regions is a particularly difficult problem because of the complexity of meteorological conditions over spatial scales ranging from individual valleys to systems of many valleys and ridges of a region, and the diurnal coupling/-decoupling phenomena between individual valleys and the regional convective boundary layer. In order to insure acceptable siting of energy development facilities in non-flat terrain, models and field measurements of the complex airflow and dispersion conditions in this complex setting must be developed and undertaken.

Dispersion, Deposition and Resuspension of Atmospheric Contaminants

Dispersion, deposition, and resuspension processes are linked intimately with the dynamics of the boundary layer. The former two processes act to reduce air concentrations of gaseous and particulate material while the latter process acts to increase air concentrations of particulate material, particularly in the large particle size classes. In many energy development areas of the West, all three processes will play an important role in determining the effective residence times of potentially hazardous particles in the atmosphere. The current program is aimed at gathering necessary field data and developing models for the prediction of the dispersion, deposition and resuspension of atmospheric contaminants.

This report describes the progress in FY 1983 for each of these generic areas. A divider page summarizes the goals of each area and lists, as bulleted items, project titles that support research in each area.

CONTENTS

CONTAMINANT CHARACTERIZATION AND TRANSFORMATION

Transformation of Energy-Related Contaminants

BOUNDARY LAYER METEROLOGY IN COMPLEX TERRAIN

Atmospheric Diffusion in Complex Terrain

Atmospheric Boundary Layer Studies

DISPERSION, DEPOSITION, AND RESUSPENSION OF ATMOSPHERIC CONTAMINANTS

Atmospheric Diffusion in Complex Terrain

Atmospheric Boundary Layer Studies

Dry Deposition

Particle Resuspension and Translocation

Theoretical Studies and Applications

Contaminant Characterization and Transformation

TRANSFORMATION OF ENERGY-RELATED CONTAMINANTS

Because of their complex chemical forms, the combustion and conversion of fossil fuels gives rise to a host of polycyclic aromatic compounds (PACs) that can be emitted into the atmosphere. A number of these PACs have been shown or are suspected to be mutagenic or carcinogenic. Once they are in the ambient air, these PACs can react with other contaminant species, such as ozone and nitrogen oxides, to form new compounds. Some of these new compounds are less mutagenic or carcinogenic than the unreacted species, while others become more so. It is thus vital that the amount and composition of these substances be characterized with respect to their source and that their subsequent transformations in the atmosphere be understood.

This year the emphasis in this project has been on measuring the effects of ozone, hydroxyl radicals and sunlight on PACs found in stack-emission plumes. Of particular interest was discovery of the inhibiting effect of nitro substituents on ozonation of PACs. This effect prevents mutagenic nitro-derivatives from degrading as rapidly as their parent compounds.

• Transformation of Energy-Related Contaminants

Objectives of this study are:

Measuring chemical transformation rates of polycyclic aromatic compounds emitted by fossil-fueled power plants.

Correlating transformation rates of these compounds with distance from the source, ambient temperature, light intensity, and concentrations of other reactant species, such as nitrogen oxides and ozone.

Evaluating the results of laboratory studies on discrete reaction steps in the overall transformation processes.

REACTION KINETICS OF POLYCYCLIC AROMATIC NITRO COMPOUNDS WITH OZONE

D. R. Kalkwarf

Polycyclic aromatic nitro compounds (PANCs) have been predicted to form on fly-ash surfaces in the stack-emission plumes from coal-fired power plants (Kalkwarf 1982). Recently, two of these compounds, 1-nitropyrene and 6-nitrobenzo[a]pyrene, were reported to be potent mutagens in human skin fibroblasts (Howard et al. 1983). Ozone reacts with many organic compounds and is continually replenished in the atmosphere. Reactions of ozone with PANCs may offer a possible mechanism for detoxifying the latter compounds provided that the rates of reaction are sufficiently rapid and that the final products are less toxic. The purpose of this study was to measure the reaction rates of representative, surface-deposited PANCs with ozone in darkness and in sunlight. The results were used to predict the half-times for ozonation of these compounds on fly ash in a stack-emission plume.

Reactions of ozone with 1-nitropyrene and with 6-nitrobenzo[a]pyrene were investigated. The apparatus for exposing these compounds to ozone and simulated sunlight is shown in Figure 1. First, a monomolecular layer of PANC was prepared on the inside surface of a 500-cm^3, round-bottom flask by a method described previously (Cope and Kalkwarf 1983). This layer was then exposed for a selected time period to a fixed concentration and flow rate of ozone gas supplied by an ozone generator (Monitor Labs, Model 8500). A flow rate of 2000 cm^3/min was used throughout this study, but the ozone concentration was varied between runs to evaluate its effect on the reaction rate. Reactions were conducted both in the dark and in 1.4 kW/m^2 of light supplied by a solar simulator (Oriel Corp., Model 6720). This is the same light intensity as the maximum light intensity that reaches the earth's surface. The reaction flask was continually rotated to illuminate the contents uniformly. The temperature of the flask was maintained at 23 ± 1°C with a water bath. After exposure, the residual PANC in the flask was extracted into methanol and then assayed by capillary-column gas chromatography using electron-capture detection.

In the dark, the amounts of 1-nitropyrene and 6-nitrobenzo[a]pyrene decreased exponentially with exposure time. Also, the pseudo first-order rate constants were proportional to the concentrations of ozone. These relationships suggest that the reaction rate could be expressed by an equation analogous to those equations reported earlier in this program for other heterogeneous reactions of the same type (Kalkwarf 1982; Cope and Kalkwarf 1983), namely:

$$\frac{-d\,(\mathrm{PANC})}{dt} = kA_m\,(\mathrm{PANC})\,[O_3]$$

where: (PANC) = amount of original PANC remaining at any time t (mol)
k = rate constant for the reaction (m/s)
A_m = molar surface area of monomolecular-layered PANC (m^2/mol)
$[O_3]$ = concentration of ozone (mol/m^3)

Rate constants calculated from the data are listed in Table 1 together with those reported earlier for reactions of ozone with the corresponding polycyclic aromatic hydrocarbons (Cope and Kalkwarf 1983). Comparison shows that the nitro group deactivated the aromatic ring systems for

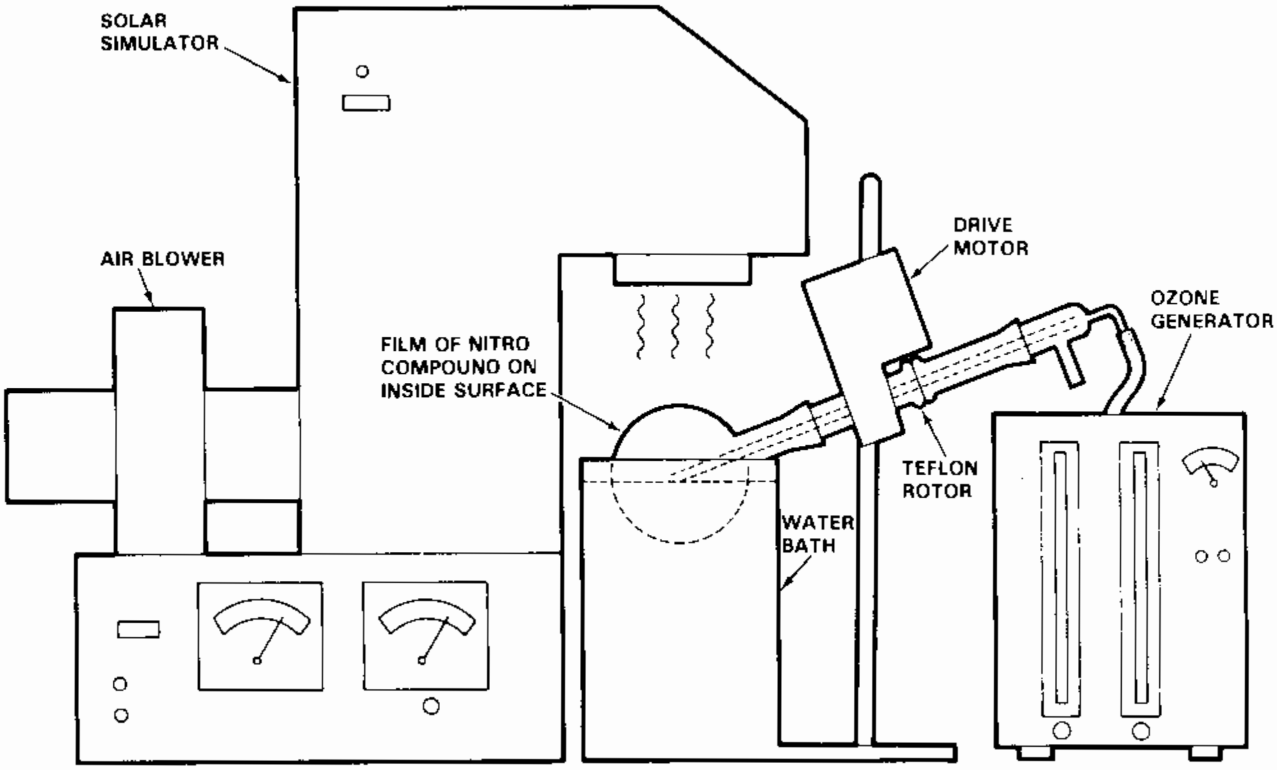

FIGURE 1. Apparatus for Exposing Surface Films of Nitro Compounds to Simulated Sunlight and Ozone.

TABLE 1 Rate Constants for Reactions of Ozone with Monomolecular Layers of Compounds Supported on Glass at 23°C in Total Darkness

Compounds	K(m/s)
PANC - 6-nitrobenzo(a)pyrene	2.1×10^{-6}
PAC - benzo(a)pyrene	6×10^{-4}
PANC - 1-nitropyrene	1.0×10^{-6}
PAC - pyrene	1.0×10^{-4}

reaction with ozone, reducing the rate constants by two orders of magnitude.

In the light, the amounts of 1-nitropyrene and 6-nitrobenzo[a]pyrene also decreased exponentially with time of exposure, but at much faster rates. Plots of the pseudo first-order rate constants for reactions of ozone with pyrene in the dark and in the light are compared in Figure 2. Both 1-nitropyrene and 6-nitrobenzo[a]pyrene decomposed in simulated sunlight even in the absence of ozone, but the dependencies of the pseudo first-order rate constants, $k_c = kA_m [O_3]$, on ozone concentration were not linear. The latter observation suggested that oxygen atoms, produced by photolysis of ozone, competed with ozone for reaction with the PANC; however, the kinetics of this potential parallel reaction have not been delineated.

To determine how ozone would react with PANCs in a stack-emission plume, their reaction half-times were calculated with a representative plume concentration of ozone, 2×10^{-6} mol/m^3 (50 ppbv). Half-time, τ, for these reactions in the dark were calculated with the following equation:

$$\tau = \frac{0.693}{kA_m[O_3]} .$$

Half-times for these reactions in the light were calculated from the pseudo first-order rate constants evaluated at 2×10^{-6} mol/m^3 ozone. The results are listed in Table 2. These results indicate that both 1-nitropyrene and 6-nitrobenzo[a]pyrene will be

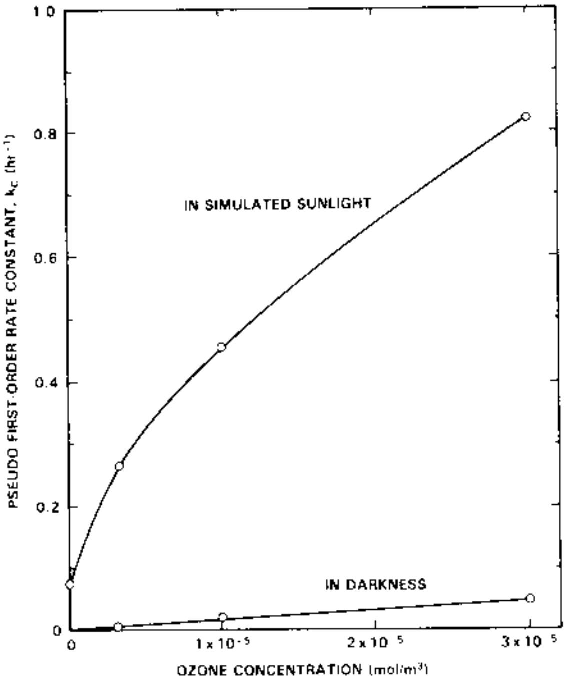

FIGURE 2. Comparison of Pseudo First-Order Rate Constants for Reactions of Monomolecular-Layered 1-Nitropyrene with Ozone in Darkness and in Simulated Sunlight.

TABLE 2. Estimated Half-Times for Reactions of Ozone with Monomolecular Layers of PANC in a Stack-Emission Plume at 23°C

PANC	A_m M^2/mol	[O_3] mol/m^3	T (dark) days	T (light)* hours
6-nitrobenzo(a)pyrene	5.8×10^5	2×10^{-6}	3	0.3
1-nitropyrene	4.4×10^5	2×10^{-6}	9	3.0

*Intensity = 1.4 kW/m^2

transformed rapidly by reactions with ozone in a stack-emission plume during daylight hours, but will be transformed very slowly at night.

References

Cope, V. H. and D. R. Kalkwarf. 1983. "Reactions Between Solid Surfaces of Polycyclic Aromatic Compounds and Ozone Gas." In Pacific Northwest Laboratory Annual Report for 1982 to the DOE Assistant Secretary for Environment, Part 3, Atmospheric Sciences. PNL-4600, PT3, pp. 2-4, Pacific Northwest Laboratory, Richland, Washington.

Howard, P. C., J. A. Gerrard, G. E. Milo, P. P. Fu, F. A. Beland and F. F. Kadlubar. 1983. "Transformation of Normal Human Skin Fibroblasts by 1-Nitropyrene and 6-Nitrobenzo[a]pyrene." Carcinogenesis 4:353-355.

Kalkwarf, D. R. 1982. "Pollutant Transformation in the Atmosphere." In Pacific Northwest Laboratory Annual Report for 1981 to the DOE Assistant Secretary for Environment, Part 3, Atmospheric Sciences. PNL-4100, PT3, Pacific Northwest Laboratory, Richland, Washington.

REACTIONS OF GASEOUS HYDROXYL RADICALS WITH POLYCYCLIC AROMATIC COMPOUNDS COATED ON GLASS

D. R. Kalkwarf and W. E. Keder

Hydroxyl radicals have been found in the troposphere at concentrations of up to 2 x 10^{-12} mol/m^3 = 10^6 radicals/cm^3 (Chameides and Davis 1982). These radicals can act as scavengers of organic pollutants and have been postulated to form as a result of the following reactions:

$$O_3 + h\nu\ (\lambda < 315\ \text{nm}) \longrightarrow O(^1D) + O_2$$

$$O(^1D) + H_2O \longrightarrow 2OH$$

Hydroxyl radicals have been shown to react rapidly with many organic compounds in the gas phase (Atkinson et al. 1979); however, no data have been reported on their possible heterogeneous reactions with solid surfaces of polycyclic aromatic compounds (PACs).

In this study, attempts were made to produce hydroxyl radicals by the photolysis of water vapor using light from a low pressure mercury lamp (Ultra Violet Products Inc., type PCQ9G-1). Only the 185-nm line from this lamp was considered energetic enough to split the water molecule (Calvert and Pitts 1966). Nitrogen gas saturated with water vapor at 0°C was passed around the lamp in the photolysis compartment of the flow system shown in Figure 1. The photolysis products were then conducted through reaction tubes coated with a monomolecular layer of pyrene or chrysene as described previously (Cope and Kalkwarf 1983).

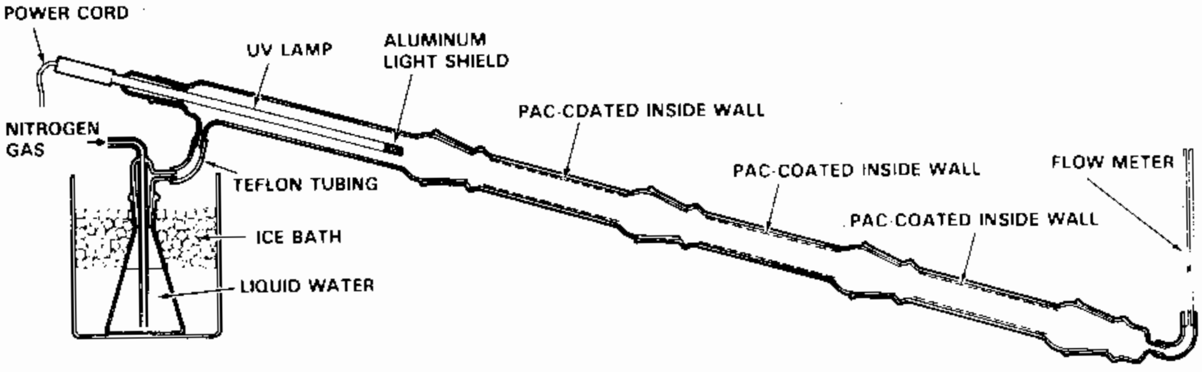

FIGURE 1. Cross-Sectional View of Apparatus for Photolysis of Water Vapor.

Photolysis of water is thought to occur by the reaction:

$$H_2O + h\nu \ (\lambda < 242 \text{ nm}) \qquad H + OH$$

Thus, hydrogen atoms are probable contaminants in the gas stream from the photolysis compartment. However, because the hydrogen atoms have a higher velocity, they should recombine at the walls of the flow system four times more rapidly than hydroxyl radicals. Thus, the monomolecular layer of PAC should have been exposed predominantly to hydroxyl radicals.

Attempts were made to evaluate the concentration of hydroxyl radicals emitted from the photolysis compartment by measuring the oxidizing ability of the gas stream. This stream was bubbled through 100-ml portions of $2.00 \times 10^{-}$ M p-nitrosodimethylaniline, a sensitive colorimetric indicator of hydroxyl radicals (Kraljic and Trumbore 1965); however, no reaction-induced bleaching of this solution was observed.

Possible reactions of PAC with hydroxyl radicals were investigated by connecting a series of coated tubes to the photolysis compartment for a measured period of time at a measured flow rate. The tubes were connected together with ground-glass joints, and the PAC was protected from light during the experiment by covering the downstream end of the lamp with aluminum foil and covering the reaction tubes with black cloth. The reaction products were removed from the tubes by washing their surfaces with methanol, compositing these washings, and evaporating them to 10-ml volumes. These solutions were then analyzed by capillary-column gas chromatography using an electron-capture detector.

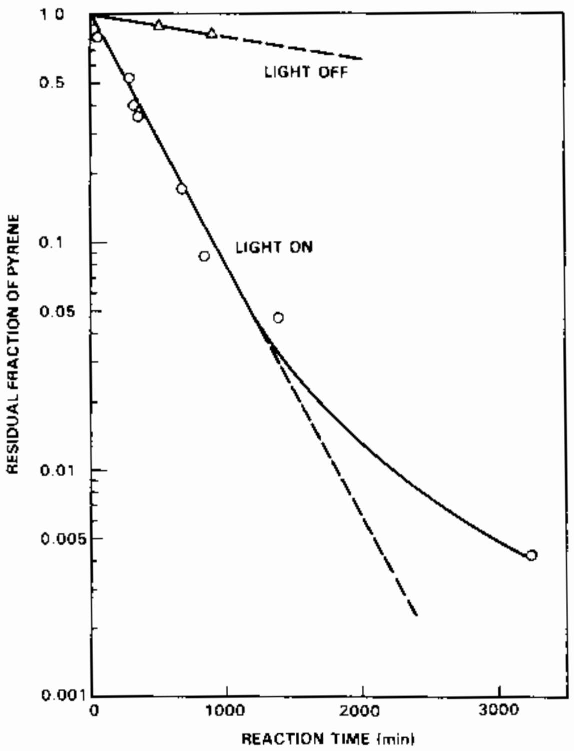

FIGURE 2. Transformation of Monomolecular-Layered Pyrene in a 1.5 mm/s Stream of Water-Photolysis Products Suspended in Nitrogen Gas.

The transformation of pyrene in the tube closest to the lamp is depicted in Figure 2. The rate was first order in the amount of pyrene, suggesting that the hydroxyl radical concentration remained relatively constant during the reaction. Some loss of pyrene was observed with the light off, and this was attributed to sublimation of pyrene into the gas stream. The rate of pyrene loss decreased progressively with increasing distance of the coated tube from the light. This indicates that the concentration of the hydroxyl radicals in the gas stream also decreased with distance from the light. Unfortunately, the concentration of hydroxyl radicals was not known, so absolute reaction-rate constants could not be evaluated. In addition to residual pyrene, three other compounds were detected by gas chromatography in extracts from the reaction tubes. These products gave much higher signals per unit weight than pyrene when the electron-capture detector was used. They also had longer retention times than pyrene on the silicone-coated chromatographic column (J & D Co., Durabond DB-5). Both of these observations suggested that the products were oxygenated derivatives of pyrene, but none were specifically identified.

Monomolecular layers of chrysene were also prepared and treated with hydroxyl radicals from the photolysis compartment. However, no decrease in the amount of chrysene was observed and no products were detected by gas chromatography even after 1000 minutes. The relative inertness of chrysene to NO_2 and O_3 was observed earlier (Kalkwarf 1982; Cope and Kalkwarf 1983). It was concluded that the hydroxyl radicals can also be a very selective reagent in transforming PACs.

References

Atkinson, R., K. R. Darnall, A. C. Lloyd, A. M. Winer, and J. N. Pitts, Jr. 1979. "Kinetics and Mechanicisms of the Reactions of the Hydroxyl Radical with Organic Compounds in the Gas Phase." In Advances in Photochemistry, Volume 11, eds. J. N. Pitts, Jr., G. S. Hammond and K. Gollnick, pp. 375-487. Wiley-Interscience, New York.

Calvert, J. G. and J. N. Pitts, Jr. 1966. Photochemistry. John Wiley & Sons, New York, New York.

Chameides, W. L. and D. D. Davis. 1982. "Chemistry in the Troposphere." Chem. Eng. News. 60(40):39-52.

Cope, V. H. and D. R. Kalkwarf. 1983. "Reactions Between Solid Surfaces of Polycyclic Aromatic Compounds and Ozone Gas." In Pacific Northwest Laboratory Annual Report for 1982 to the DOE Assistant Secretary for Environment, Part 3, Atmospheric Sciences. PNL-4600, PT3, pp. 2-4, Pacific Northwest Laboratory, Richland, Washington.

Kalkwarf, D. R. 1982. "Pollutant Transformation in the Atmosphere." In Pacific Northwest Laboratory Annual Report for 1981 to the DOE Assistant Secretary for Environment, Part 3, Atmospheric Sciences. PNL-4600, PT3, pp. 15-17, Pacific Northwest Laboratory, Richland, Washington.

Kraljic, I. and C. N. Trumbore. 1965. "p-Nitrosodimethylaniline as an OH Radical Scavenger in Radiation Chemistry," J. Am. Chem. Soc. 87:2547-2550.

EFFECT OF SUNLIGHT ON REACTION RATES OF OZONE WITH PYRENE AND PYRENE QUINONES

V. H. Cope and D. R. Kalkwarf

Past results suggest that certain polycyclic aromatic hydrocarbons (PAHs) are chemically transformed at significant rates by reactions with ozone, even in total darkness (Cope and Kalkwarf 1983). This report describes experiments to measure the effect of simulated sunlight on the reaction rates of ozone with a representative PAH, pyrene, and with a mixture of its major ozonation products, pyrene-1, 6-quinone and pyrene-1, 8-quinone. The purpose was to estimate the transformation half-times of these substances in stack-effluent plumes exposed to both intense sunlight and ambient ozone.

Monomolecular layers of pyrene and the pyrene quinones were prepared on the inside surfaces of 500-cm^3 round-bottom flasks by a method described previously (Cope and Kalkwarf 1983). The layers were exposed to ozone and simulated sunlight with the apparatus described previously (p. 1). The light intensity was adjusted to 1.4 kW/m^2, which is the maximum intensity of light striking the earth's surface. After exposure for selected time periods to a fixed concentration and flow rate of ozone, the layers were dissolved in methanol and analyzed by high-performance liquid chromatography.

The amount of pyrene and the amount of each quinone decreased exponentially with exposure time. The rate of decrease was proportional to the concentration of ozone. The molar ratios of the quinones remained constant indicating that both isomers reacted at the same rate. The loss of pyrene by reaction was corrected for the small loss due to sublimation. In each case, the transformation rate of the compound could be represented by the equation:

$$-\frac{d(PAC)}{dt} = kA_m \, (PAC) \, [O_3]$$

where: (PAC) = amount of original polycyclic aromatic compound remaining at any time t (mol)

k = rate constant for the reaction (m/s)

A_m = molar surface area of monomolecular-layered PAC (m^2/mol).

Rate constants evaluated for reactions in simulated sunlight and in darkness are listed in Table 1. Comparison shows that simulated sunlight had only a slight effect on the rate constant for ozone and pyrene, but it enhanced the rate constant for reactions between with the pyrene quinones 15-fold.

TABLE 1. Rate Constants for Reactions of Ozone with Monolayers of Compounds Supported on Glass at 23°C in Darkness or in Simulated Sunlight at an Intensity of 1.4 kW/m²

Compound	k(M/s) in Darkness	k(m/s) in Sunlight
pyrene	1.0×10^{-4}	1.3×10^{-4}
pyrene-1,6-quinone	2.0×10^{-5}	3.0×10^{-4}
pyrene-1,8-quinone	2.0×10^{-5}	3.0×10^{-4}

The transformation half-times, τ, of these compounds in a stack-emission plume were estimated from the following equation:

$$\tau = \frac{0.693}{kA_m[O_3]}$$

using a typical ozone concentration of 2×10^{-6} mol/m^3 (50 ppbv). The results are shown in Table 2.

TABLE 2. Estimated Half-Times for Reactions of Ozone with Monomolecular Layers of PAC in a Stack-Emission Plume at 23°C

PAC	A M²/mol	[O₃] mol/m³	T (dark) hours	T (light) hours
pyrene	4.4×10^{5}	2×10^{-6}	2	2
pyrene-1,6-quinone	4.4×10^{5}	2×10^{-6}	11	0.7
pyrene-1,8-quinone	4.4×10^{5}	2×10^{-6}	11	0.7

It was concluded that exposure to sunlight would have very little effect on the rate of transformation of pyrene on airborne fly ash in stack-emission plumes, but the product quinones would be rapidly transformed to other products whose identities are yet unknown.

References

Cope, V. H. and D. R. Kalkwarf. 1983. "Reactions Between Solid Surfaces of Polycyclic Aromatic Compounds and Ozone Gas." In Pacific Northwest Laboratory Annual Report for 1982 to the DOE Assistant Secretary for Environment, Part 3, Atmospheric Sciences. PNL-4600, PT3, pp. 2-4, Pacific Northwest Laboratory, Richland, Washington.

Boundary Layer Meteorology in Complex Terrain

BOUNDARY LAYER METEOROLOGY IN COMPLEX TERRAIN

- **Atmospheric Diffusion in Complex Terrain**
- **Atmospheric Boundary Layer Studies**

Major reserves of fossil fuels are located in mountainous or other complex terrain. As the use of these fuels as an energy source increases, the emission of air contaminants, such as sulfur and nitrogen compounds, trace metals, and fugitive dust produced by the combustion, conversion, and extraction of these fuels, will increase also. The analysis of the fate of these pollutants is particularly difficult in mountainous terrain settings, but is urgently needed to insure that the nation's energy plan can proceed efficiently and yet be environmentally sound.

The research activities at PNL are related to the interlaboratory Atmospheric Studies in Complex Terrain (ASCOT) program. A wealth of data from the Geysers area is being analyzed and tested against a variety of models accounting for the transport and dispersion of air contaminants under nocturnal meteorological conditions. Contributions were made to an interlaboratory report summarizing ASCOT progress on the analysis and modeling of data collected during the first three years of the program. During FY 1983, the area of study focus shifted from the Geysers Geothermal Site in California to the oil shale region in western Colorado. An effort is being made to determine how much of the experience gained at the Geysers can be extended to the oil shale regions of Colorado.

The field activities in the ASCOT program include the micrometeorological description of drainage winds from data obtained at Hanford (Rattlesnake Mountain), the Geysers (Anderson Creek, Big Sulfur Creek), and Colorado (Brush Creek). Other tasks include analyzing energy and mass budgets and evaluating transport and diffusion of contaminants by using tracer experiments. In preparation for the 1984 ASCOT field program in Colorado, new measurement systems are being developed including remote wind sensing with Doppler sodar and high frequency turbulence measurement with sonic anemometers.

• Atmospheric Diffusion in Complex Terrain

Objectives of this study are:

Developing and evaluating a long-range technical plan for studying the transport and diffusion of contaminant particles and gases over complex landforms.

Assisting a multilaboratory program studying diffusion in complex terrain by providing methodologies and techniques for analyses of transport and diffusion over a variety of complex landforms.

Developing and evaluating various transport and dispersion models for complex terrain.

TEMPERATURE INVERSION BUILDUP AND DECAY ON A MOUNTAIN SLOPE

M. M. Orgill

The PNL ASCOT group has been using the ASCOT data base to examine the effect of large-scale (synoptic and mesoscale) wind systems on the development and persistence of local winds at the Geysers Geothermal area. These analyses are a continuation of past work reported by Orgill, Schreck and Whiteman (1981) and Orgill (1983). Further results have been summarized in an article to the Bulletin of the American Meteorological Society, which is under review for publication.

This report examines the problem of how large-scale wind systems can disturb the temperature inversion (stable) layer that forms over the slope in the Anderson-Putah Creek area in the Geysers. Figure 1 shows a cross-section of the temperature inversion structure over the Anderson Creek slope in July 1979. Nocturnal or radiational cooling always produced surface and elevated temperature inversions over the Anderson Creek area. The temperature inversion structure usually consisted of a lower-level inversion about 50 to 200 m deep, an upper isothermal layer, and a second inversion layer about 400 m above the slope. On 'good' drainage wind nights, the drainage wind layer on the slope of Anderson Creek appears to be about 2 to 3 tenths of the total stable layer (top of the highest temperature inversion). Generally, the depth of both the inversion and the drainage layer would increase with distance downslope.

Analysis of data from the July 1979 and September 1980 experiments indicates that the stable inversion layer was subjected to strong (6 m/s or more) upper-level westerly or easterly winds. This resulted in the erosion of the stable layer on the slope.

Table 1 shows the hourly potential temperature gradient in the lowest 100 m for the experimental nights of September 1980. The table shows that a stable layer formed on all experiment nights. On three experimental nights (September 15-16, 21, and 22) upper-level easterly winds descended over the slope resulting in the erosion of the stable layer from above. On September 18-19, strong westerly winds in the early evening delayed the formation of the stable layer. On two nights (September 21 and 22) the easterly winds were very persistent and caused the stable layer to disappear on the slope thus terminating the drainage wind and the planned tracer experiments.

Figure 2 compares the height of the stable layer for two different nights in September 1980. The night of September 19-20 was generally classified as one of the better drainage wind nights. The upper-level winds above ridge tops were generally from the northwest at 1 to 3 m/s. As shown in Figure 2, the stable layer during this night was present over the ridge, slope and valley. On the night of September 15-16, the stable layer, on the average, was lower in height at all locations as the result of easterly winds descending during the evening. At Unit 19, between 1800 and 2300 PST the upper-level easterlies descended from 300 m to about 25 m at a rate of about 55 m/hr. The easterlies remained below 25 m between midnight and 0300 PST until rising to 50 m around 0600 PST. The time variation in height difference of the stable layers for the two nights is shown in the upper part of Figure 2. The stable layer on the night of September 15-16 started to form in the early evening, but after 20 PST the easterlies had started to descend over the slope and the stable layer decreased in height (>-400 m) when compared to the undisturbed night of September 19-20.

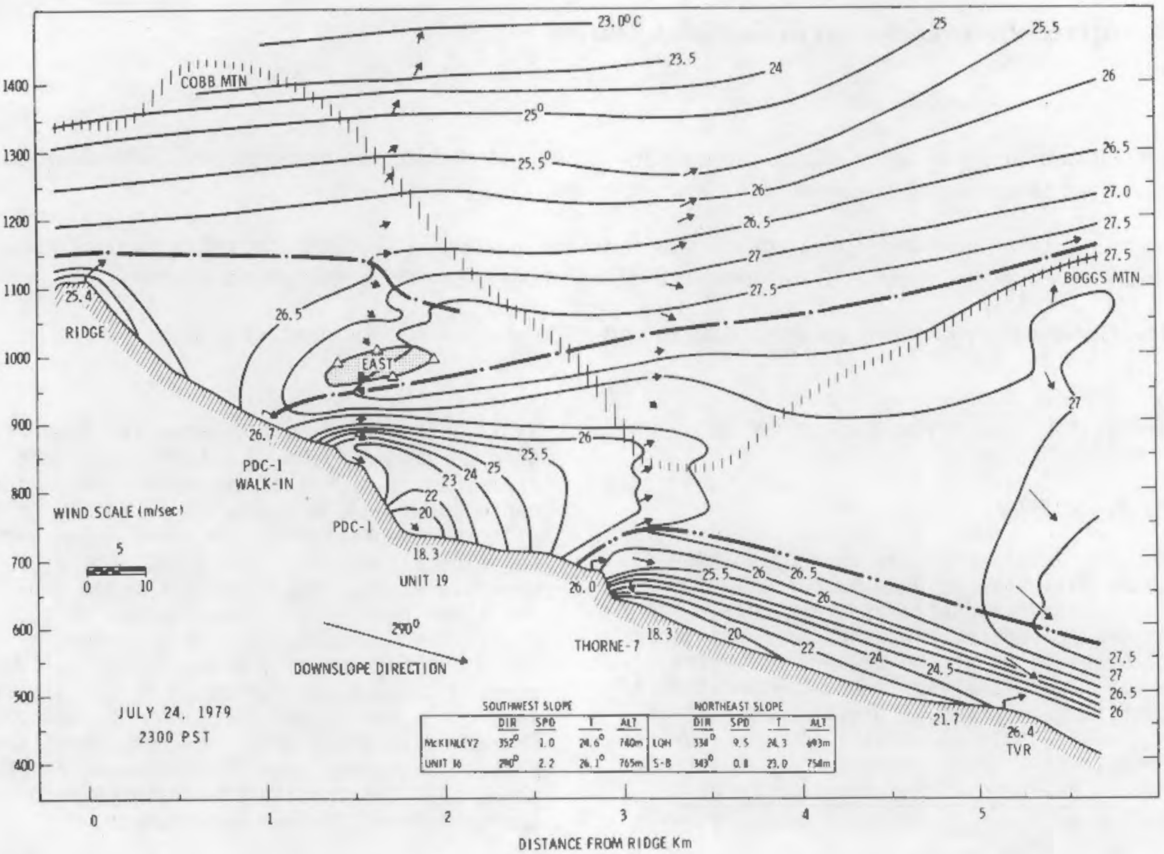

SOUTHWEST SLOPE	DIR	SPD	T	ALT	NORTHEAST SLOPE	DIR	SPD	T	ALT
McKINLEY2	352°	1.0	24.6°	740m	LQH	338°	9.5	24.3	493m
UNIT 16	290°	2.2	26.1°	765m	S-B	343°	0.8	23.0	754m

FIGURE 1. Temperature Inversions (heavy dash-dot lines), Winds and Isotherms (C) for 2300 PST July 24, 1979. View looking to the north. Hatched vertical line is topographic profile of Cobb Mtn. and Boggs Mtn in the background.

TABLE 1. Hourly Potential Temperature Gradients in the Lowest 100 m at Unit 19 During September 1980 (°C/m)

	Hour (PST)															
Date	16	17	18	19	20	21	22	23	00	01	02	03	04	05	06	07
Sept. 11-12			0.02	0.06	0.06	m	0.10	0.11	0.11	0.10	0.08	0.11	0.09	0.09	0.08	
Sept. 15-16			0.03	0.04	0.08	0.08	0.08	0.09	0.10	0.05	0.07	0.10	0.09	0.09	0.10	
Sept. 18-19			0	0.01	0	0.01	0	0.03	0.03	0.03	0.05	0.05	0.05	(Storm night)		
Sept 19-20				0.02	0.05	0.06	0.07	0.08	0.07	0.07	0.07	0.08	0.07	0.08	0.08	0.07
Sept. 21		0.03	0.04	0.08	0.09	0.02	(Easterlies)									
Sept. 22			0.10	0.10	0.09	0.12	(Easterlies)									
Sept. 24-25	0	0.04	0.05	0.10	0.10	0.09	0.11	0.11	0.11	0.11	0.12	0.12	0.11	0.11	0.10	0.08

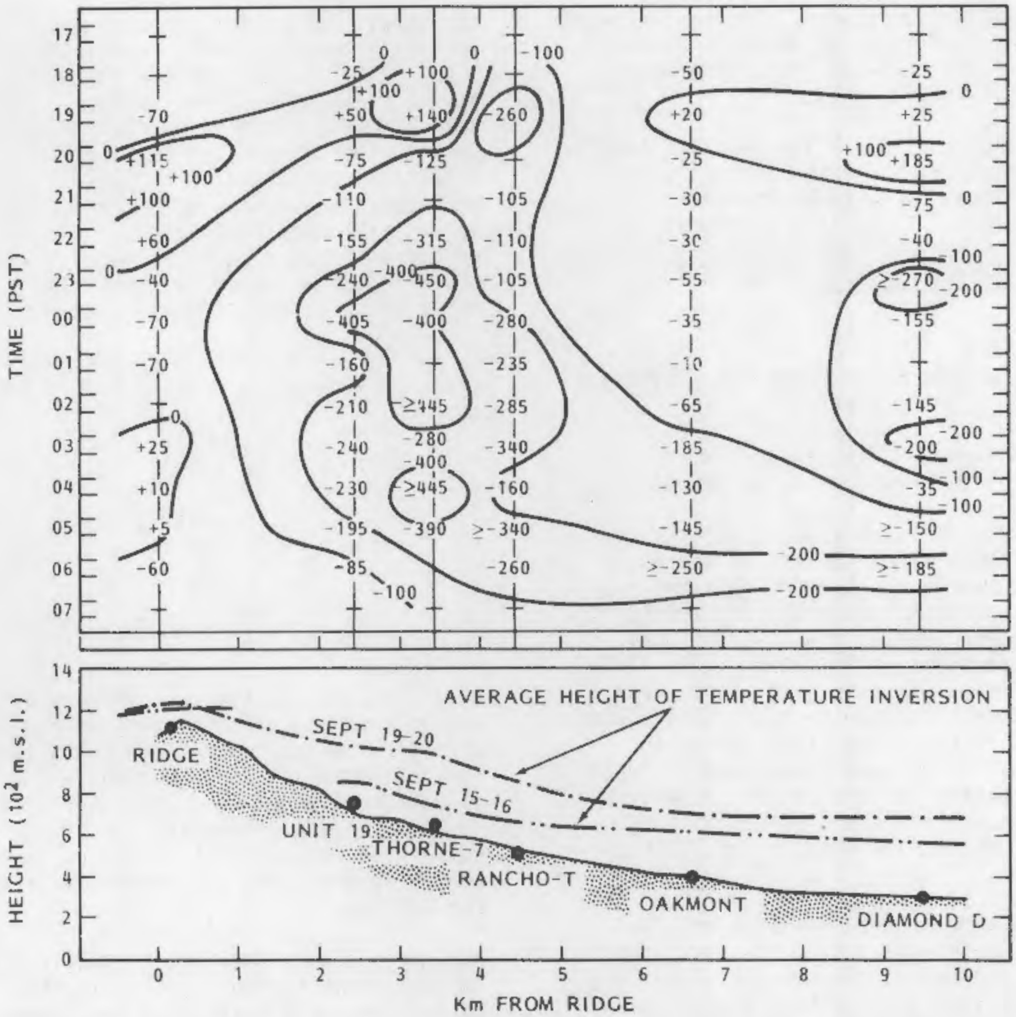

FIGURE 2. (Top) Time Variation of the Stable Layer Height Differences Between September 19-20 and September 15-16, 1980 (H15-16, H19-20). (Bottom) Cross-Sectional View of the Average Height of the Stable Layer for the Same Two Dates.

The possible mechanisms for causing these space and time variations in the drainage winds and temperature inversions is under investigation by ASCOT investigators. Two mechanisms that appear to account for the time and height variation in the stable layer in September 1980 are topographically driven buoyancy waves and dynamic instabilities. Acoustic sounder records from the Wave Propagation Laboratory (WPL) in Boulder, Colorado, provide evidence for both types of mechanisms.

The nights of September 15-16, 21, and 22 are good examples where these two mechanisms were either competing or cooperating in dissipating the temperature inversion and drainage wind. On at least two of these nights (September 21 and 22), the rate at which the easterly winds descended into the valley is consistent with a resonant lee wave length and a microscale erosion by dynamic instability (due to wind shear and turbulence) at the top of the stable layer. These cases and others will be studied in greater depth in an attempt to verify the role of these mechanisms in dissipating drainage layers in the Geysers area.

References

Orgill, M. M., R. I. Schreck and C. D. Whiteman. 1981. "Synoptically Driven Downslope Winds and Their Effects on Local Nocturnal Drainage Airflow in the Geysers

Geothermal Resource Area." Paper presented at Second Conference on Mountain Meteorology, November 9-11, 1981, Steamboat Springs, Colorado.

Orgill, M. M. 1983. "Synoptic and Local Scale Interactions in the Geysers Geothermal Resource Area--An Overview," PNL-4600 PT3. In Pacific Northwest Laboratory Annual Report for 1982. Part 3. Atmospheric Sciences, pp. 11-13.

BUDPLT - A COMPUTER PROGRAM FOR ESTIMATING ENERGY BUDGETS IN VALLEYS

C. D. Whiteman, R. I. Schreck, M. M. Orgill, T. W. Horst and G. A. Sehmel

The problem of temperature inversion evolution in mountainous valleys is currently unsolved due to the lack of relevant measurements and the technical difficulty of the problem. During the Environmental Protection Agency-DOE (GRAMA-ASCOT) field program in July-August 1982, an important data base of tethersonde measurements were obtained in the Brush Creek Valley in Colorado. These data appear nearly ideal for evaluating the problem of temperature inversion evolution and determining the physical mechanisms responsible for this evolution.

Three PNL-DOE programs and one PNL-EPA program cooperated during the last year to develop a computer program for evaluating various physical mechanisms responsible for temperature inversion development and dissipation in a valley. The program currently being used is BUDPLT, an interactive FORTRAN program for evaluating energy budget terms.

The theoretical approach involves combining the First Law of Thermodynamics and the Euler Equation for temperature changes into the following equation,

$$\frac{\partial T}{\partial t} = \frac{1}{c_p}\frac{dQ}{dt} - u\frac{\partial T}{\partial x} - v\frac{\partial T}{\partial y} - w\left(\frac{g}{c_p} - \gamma\right) \qquad (1)$$

where:
T = temperature
t = time
Q = specific energy supplied by diabatic processes such as radiation, evaporation, and condensation
c_p = the specific heat of air at constant pressure
u,v,w = the wind components
g = the acceleration due to gravity
γ = the temperature lapse rate.

The energy budget for the air volume of a valley can be obtained by multiplying Equation (1) by ρc_p and integrating over the volume of a valley cross-section. The valley volume would be defined using the valley floor width, the slope of the two sidewalls, the width of the valley cross-section at the height of the inversion top, and an arbitrary depth given, for example, by the distance between tethered balloon profiling sites along the valley axis. The terms of Equation (1) would then become:

$$\begin{aligned}\iiint \rho\, c_p \overset{(A)}{\frac{\partial T}{\partial t}}\, dxdydz &= \iiint \rho \overset{(B)}{\frac{dQ}{dt}}\, dxdydz \\ &- \iiint \rho\, c_p\, u \overset{(C)}{\frac{\partial T}{\partial x}}\, dxdydz \\ &- \iiint \rho\, c_p\, v \overset{(D)}{\frac{\partial T}{\partial y}}\, dxdydz \\ &- \iiint \rho\, c_p\, w \overset{(E)}{\left(\frac{g}{c_p} - \gamma\right)}\, dxdydz\end{aligned} \qquad (2)$$

Term A identifies the loss or gain of energy from the valley volume as the temperature inversion develops or dissipates. Term B identifies the contribution of the diabatic processes to energy loss or gain. Terms C, D, and E identify the effects of horizontal and vertical advection on the energy loss or gain of the volume of air in the valley.

The present data base for evaluating the various terms in Equation (2) is the tethersonde data taken in Brush Creek. This limits the computer program to evaluating Terms A, C and D, because w (vertical motion) and Q were not measured in that field program.

The BUDPLT program is being used to evaluate the tethersonde data from Brush Creek. The program performs double and triple integrations of one or two variables and can integrate with time or distance. If the user is using a computer terminal that has graphics capabilities, he may plot optionally the input integrand variables versus height before the integration is started. A plot file of the integral output, which can be implemented on different graphics devices, is always created.

The program prompts the user to enter the number of tethersonde sites for which profiles are to be integrated. A list of the sites is displayed on the terminal screen and the user may select one or two sites. A list of dates, times, and maximum heights of the profiles is displayed for the sites selected. The user is then prompted for the profile number to be integrated, the maximum height of the integral, and the height increment of integration. A list of integrand variables is displayed, and the program asks the user to select up to two variables. Integral scalar multipliers or divisors may also be selected. An output plot file, a listing file of input variables, and integral values are created by the program. After each integral is completed, the program loops back to the beginning and asks the user whether another integral is to be calculated.

The BUDPLT program is currently being checked for errors and will undergo evaluation tests in the near future. The first application of the program will be for the Brush Creek area of Colorado.

• Atmospheric Boundary Layer Studies

Objectives of these studies are:

Investigating the meteorological characteristics of the planetary boundary layer that pertain to contaminant transport and dry removal.

Analyzing the transport and diffusion of contaminants in complex terrain, particularly in the Geysers Geothermal Area of California and the western slope of the Rocky Mountains in Colorado.

Constructing simple models for the prediction of the depth, speed, and direction of gravity-controlled drainage flows and of turbulence and contaminant dispersion within these flows.

TURBULENCE STRUCTURE OF DRAINAGE WINDS OVER A SIMPLE SLOPE

J. C. Doran and T. W. Horst

Under stable conditions, turbulent kinetic energy is generated solely by mechanical shear because there is no buoyant production. Since the mean wind profiles found in drainage winds are significantly different from those found over flat terrain, the turbulent energy profiles are likely to also be affected. This could, in turn, have important ramifications for the dispersion of pollutants released into such an environment.

We made a preliminary investigation of this effect by analyzing the data from observations of drainage winds during two nights on Rattlesnake Mt. The first night was July 1 to 2, 1980; during the period of interest the ambient winds were generally downslope. Ambient winds combined with katabatically induced winds to produce a well-defined jet in the downslope wind component with the peak wind speed occurring at a height of approximately 2 m. Immediately above and below this height, the wind shears were relatively large, but at greater heights the wind speed changed more slowly.

In contrast to this case, on the night of July 2 to 3, 1981 ambient winds were upslope and cross slope. The resultant wind speed profile showed a weak jet in the downslope component with a peak slightly below 2 m, and considerable shear in both speed and direction above this height.

The substantially different shears in these two cases suggest that the turbulent kinetic energy profiles should also differ. Power spectra of the downslope component of the wind were computed to examine this possibility. For both cases, the spectra could be divided into two regions. Below a frequency of approximately 0.02 Hz, the spectra are more suggestive of wave motion; above this value, the spectra order in a manner consistent with the assumed generation of turbulence by wind shear. Figure 1 shows spectra for the 1981 case. There is a monotonic increase of the turbulent kinetic energy with height; a condition that is precisely the reverse of that expected in stable conditions over flat terrain. For the 1980 case, the spectra do not order so neatly, reflecting the more complicated shear profile. The observed behavior on both nights is consistent with the results obtained from numerical simulations with a 1-dimensional model developed earlier in this program (Doran and Horst 1983).

The combination of sloping terrain, stable conditions, and varying ambient wind direction apparently can substantially complicate the turbulent structure of the atmosphere. Such effects may have to be explicitly taken into account to properly describe the transport and diffusion of atmospheric pollutants, and the coupling of near-surface winds to winds aloft.

COMPARISON OF WINDS MEASURED BY DOPPLER SODAR AND HMS 120 METER TOWER

G. F. Athey and T. W. Horst

A Radian Echosonde III doppler acoustic sounder has been acquired for use in field studies in complex terrain. The system consists of three monostatic antennas with two of them tilted at 18 degrees from vertical to obtain the horizontal winds. The sodar measures the three wind components to a nominal height of 600 m and returns echo intensities to a nominal height of 1000 m.

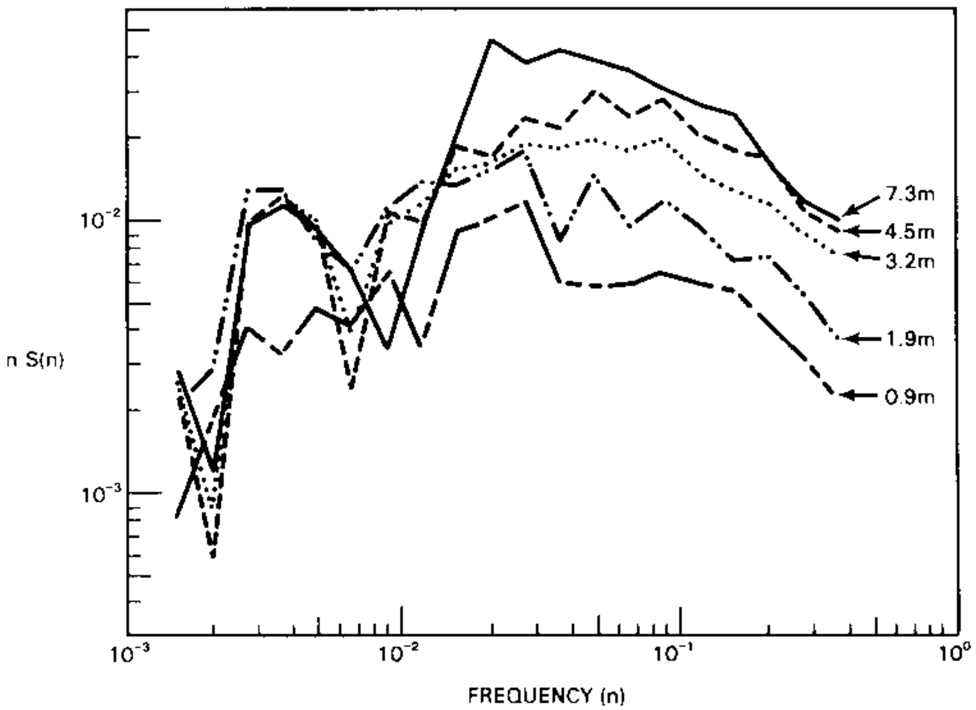

FIGURE 1. Spectra of 1981 Data

A comparison of the winds measured by doppler sodar and by the Hanford Meteorological Station tower was made during early 1983. Hourly data were collected over a 12 day period from February 18 through March 1. The primary purpose of the comparison was to evaluate the operation of the doppler sodar.

Measurements were made at four levels: 30.5, 61.0, 91.5, and 121.9 meters. The tower measures winds by using cup and vane anemometers located at the selected levels and displays the analog signals on strip-charts. The hourly values of speed and direction are derived from visual inspection of the analog signal. The forecaster records an estimate of the hourly wind speed to the nearest mph and the prevailing direction to the nearest 10 degrees. The doppler sodar sends out an acoustic beam in preset configurations. Wind components parallel to the beam are determined by measuring the doppler shift of the scattered sound. The measured winds during the test were based on doppler gates 15.2 meters wide centered on the 4 levels. Hourly averages are based on continual sampling over the hour and are reported to the nearest tenth in meters per second and degrees.

Table 1 shows a comparison of the wind speeds measured by the tower and the sodar. The table shows good agreement between the measurements with the exception of measurements taken at the 30.5 meter level. The similarity of the standard deviations suggests that the instruments are seeing the same processes. The results indicate that the sodar is doing a reasonable job of measuring the wind speed above about 45 meters.

Table 2 gives a summary of the differences between the measured wind speeds and directions. Each hourly tower measurement was subtracted from the doppler measurement and the differences analyzed. Positive direction differences represent clock-wise rotation; negative differences are counter clock-wise.

TABLE 1. Mean Wind Speeds and Standard Deviations in m/s for Sodar and Tower

	Sodar		Tower	
	Mean	SD	Mean	SD
30.5	2.32	1.34	3.92	1.83
61.0	4.30	2.32	4.42	2.24
91.5	4.70	2.59	4.59	2.49
121.9	4.59	2.61	4.63	2.53

TABLE 2. Wind Speed and Direction Differences (Sodar - Tower)

	Speed (m/s)		Direction	
	Mean	SD	Mean	SD
30.5	-1.61	1.71	-11.43	65.85
61.0	-0.11	0.70	11.15	28.36
91.5	0.12	0.67	4.15	22.50
121.9	-0.04	0.74	6.05	18.71

Again, with the exception of the lowest level, the results suggest that the sodar is accurately measuring the winds. The problem at the low level may be due to a "ringing" problem associated with the vertical transducer. The sodar vertical velocities for that level were often too high. The vertical component is subtracted from the winds measured by the tilted antenna to obtain the horizontal components. Thus, when the vertical leg has high values, the computed horizontal winds will be low.

Because we cannot digitally record data from the tower at this time, it is not reasonable to conduct further analysis. Also, there are inherent differences in the way in which the winds are measured. The anemometers measure flow at a fixed point. The sodar measures a volume average and has a minimum height resolution.

Future plans for improving and testing the operation of the doppler sodar include:

1. eliminating transducer ringing problems
2. a more precise alignment of antennas
3. digital recording of tower winds and further comparison tests against the tower, and
4. a comparison test against the time-of-flight laser anemometer (TFLA) being developed at PNL.

ASCOT PROGRESS ON DRAINAGE FLOW OVER SIMPLE SLOPES

T. W. Horst and J. C. Doran

In 1981 the DOE interlaboratory ASCOT (Atmospheric Studies in Complex Terrain) program completed three years of field studies in the Geysers Geothermal Resource Area of northern California. These measurement programs and concurrent ASCOT model development have focused on understanding the dynamics of nocturnal drainage flows and the transport and dispersion of pollutants within these flows. Analysis of the Geysers data and modeling of the atmospheric flows in the Geysers study areas have progressed sufficiently to warrant a progress report on this first phase of the ASCOT program. This report was written by the participating laboratories during the past year and covers three areas: Physical Concepts, Measurement Programs, and Modeling Studies.

One focus of ASCOT research at PNL has been drainage flow on simple slopes. Understanding this initial phase of drainage flow is essential to a realistic prediction of the scales and occurrence of drainage winds. Accordingly, the present authors were selected to write Section 3.2 of the ASCOT Progress Report, Nocturnal Drainage Flow on Simple Slopes (PNL-SA-11245). The conclusions of this chapter are summarized below.

Measurements of nocturnal drainage flow have been made at a large number of sites during the ASCOT program, but only a few of these are suitable for study of drainage flow on simple slopes. This report is based largely on data from Geysers Unit 19 and Rattlesnake Mountain because detailed, continuous profiles of wind and temperature were measured at these sites with tower-mounted instruments. At the Rattlesnake Mountain site, measurements were made at several distances from the top of a simple, grassy slope; at the Geysers Unit 19 site, a single tower was located in a more complex, tree-covered basin.

Nocturnal drainage flow on a simple slope is driven by a surface inversion with a depth of about 0.05 of the vertical drop from the top of the slope. At the Geysers Unit 19 site, 670 m below the summit of Cobb Mountain, the inversion depth averaged 45 m, its strength was typically 10°C, and the corresponding layer-integrated katabatic acceleration was 0.5 m^2/s^2. Tower B at the Rattlesnake Mountain site is only 150 m below the ridge top and hence the scales of the slope flow were smaller: an inversion depth of 4 to 8 m, a typical inversion strength of 3°C, and a katabatic acceleration of 0.05 m^2/s^2.

At the Geysers site, the wind direction within the cooled inversion layer was essentially downslope and a low-level maximum wind speed of 1 to 2 m/s occurred at a height that was 0.4 to 0.5 times the inversion depth. The wind direction shifted from downslope at a height of 0.8 to 0.9 times the inversion depth. At the Rattlesnake Mountain site, the ambient winds had a strong influence near the surface and thus the low-level winds were seldom downslope. However, the downslope component of the wind exhibited a low-level maximum at a height that was 0.4 times the inversion depth, and when the ambient winds were light, with a typical magnitude of 1 to 2 m/s.

The surface inversion depth, the height of a wind direction shift from downslope, and the height above the jet of a wind speed minimum are all measures of the depth of the layer that is influenced by katabatic flow. Some evidence suggests that these depths may be similar for a simple slope, but it is also apparent that the measures based on the wind profile above the jet are dependent on the ambient wind speed and direction.

Two additional depth scales, the momentum depth and the temperature deficit depth, are defined by vertical integrals of the wind and temperature profiles. These have the advantage that they do not depend on identifying the height of occurrence of a particular feature of the profiles. However, their definition is ambiguous if the wind speed or temperature deficit do not go to zero above the katabatic flow. The momentum depth is roughly equal to the depth of the surface inversion, and the temperature deficit depth is about one-fourth of the inversion depth. The temperature deficit depth is easier to determine, because the temperature deficit is more likely than the wind to approach zero at the top of the katabatic layer and it appears to be less sensitive to ambient wind and stratification.

The strength and vertical scale of slope flow increase with downslope distance due to cooling at the surface and entrainment of ambient air at the top of the flow. The inversion becomes deeper and stronger, and the maximum downslope wind speed, the height of the wind maximum, and the total depth of downslope flow increase. The vertical scales of the flow increase linearly with distance down a constant slope, and the strength of the inversion and the downslope wind speed increase at a lesser rate.

Predictions of the momentum depth as a function of slope angle and downslope distance using Ellison and Turner's (1959) laboratory-measured entrainment rates agree well with observations of the approximately equivalent inversion depth. For moderate slopes these entrainment rates are roughly proportional to the sine of the slope angle, and hence the growth of the vertical scales is roughly proportional to the vertical drop from the top of the slope, e.g., the inversion depth is about 0.05 times the vertical drop.

The vertical distribution of turbulence is quite different in slope flow than in stable conditions over flat, homogeneous terrain. This is a consequence of the shear distribution associated with the low-level wind maximum. Local shear production of turbulent energy decreases with height, reaches a local minimum at the height of the jet, and then increases once more. Above the jet, the profiles of shear and turbulent energy depend on the magnitude and direction of the ambient wind. Ambient winds that are upslope or cross-slope produce more shear above the jet, and consequently more turbulence, than downslope ambient winds.

Several of the features of nocturnal slope flow are useful indicators of its occurrence. These are the surface-based inversion, the low-level wind maximum and the downslope wind direction. The surface inversion is necessary for slope flow, but the wind maximum and the downslope direction may be obscured by ambient winds, particularly at an exposed site. A downslope wind direction and small values of σ_θ were found to be good indicators of slope flow in the sheltered Anderson/Gunning Creek Basin; however, at the Rattlesnake Mountain site it was necessary to look for a low-level maximum in the downslope wind component because ambient winds strongly influenced the wind profile at the surface.

The best slope flows occur on calm nights with clear skies that allow the development of a strong surface inversion. Good slope flows at the Geysers Unit 19 site required ridge-top wind speeds of less than 6 m/s and a surface inversion strength above 5 m of at least 5°C. The ridge-top wind speed, the strength of the inversion and the inversion depth can be combined to form a slope Richardson number (Ri) that correlates well with the occurrence of slope flow. Most of the good slope flow at the Unit 19 site occurred when $Ri > 0.7$; good slope flow never occurred when $Ri < 0.2$ and no drainage occurred when $Ri < 0.15$.

The onset, maintenance, and breakup of slope flow is similarly dependent on the establishment, maintenance and destruction of the surface inversion. Although the soil and the near-surface air begin to cool well before local sunset, strong downslope flow begins only after the ambient wind is weak enough to permit formation of an inversion adequate to drive the flow. Even after good slope flow has been established, however, it can easily be disrupted by increased winds that weaken the inversion and reduce the katabatic force by turbulent mixing. The slope flow is also terminated rapidly at local sunrise by the heating of the surface and the subsequent destruction of the surface inversion.

The dependence of slope flow structure on ambient conditions varies from site to site. The Rattlesnake Mountain site was very exposed and hence the wind profile was strongly influenced by the ambient winds. Only the depth of the surface inversion and the height of the downslope wind maximum were relatively insensitive to ambient conditions. The Geysers Unit 19 site was more protected and both the wind and temperature profiles were less sensitive to ambient conditions. However, a decrease with time of the speed and depth of the downslope flow at this site appears to be correlated with an increase in ambient stratification. It is postulated that the increasing stratification of the air above the slope isolates the katabatic layer from the flow aloft and produces a weaker near-surface flow driven only by katabatic forces.

References

Ellison, T. H., and J. S. Turner. 1959. "Turbulent Entrainment in Stratified Flows." J. Fluid Mech. 6:423-448.

Horst, T. W., and J. C. Doran. 1983. Nocturnal Drainage Flow on Simple Slopes - An ASCOT Progress Report. PNL-SA-11245, Pacific Northwest Laboratory, Richland, Washington.

Dispersion, Deposition and Resuspension of Atmospheric Contaminants

DISPERSION, DEPOSITION AND RESUSPENSION OF ATMOSPHERIC CONTAMINANTS

- **Atmospheric Diffusion in Complex Terrain**
- **Atmospheric Boundary Layer Studies**
- **Dry Deposition**
- **Particle Resuspension and Translocation**
- **Theoretical Studies and Application**

The concentration of contaminant species in air is governed by the rate of input from sources, the rate of dilution or dispersion as a result of air turbulence, and the rate of removal to the surface by wet and dry deposition processes. Once on the surface, contaminants also may be resuspended, depending on meteorological and surface conditions. An understanding of these processes is necessary for accurate prediction of exposures of hazardous or harmful contaminants to humans, animals, and crops.

At PNL several research programs focus attention on these processes through a combination of field, laboratory and modeling studies. In the field, plume dispersion and plume depletion by dry deposition are studied by the use of tracers. A unique application of tracer technology at PNL is the simultaneous release of depositing and non-depositing tracers. Dry deposition was investigated for particles of both respiration and inhalation interest. Studies are being conducted to evaluate simple plume depletion models and resuspension-diffusion-deposition models have been applied to estimate pesticide concentrations above treated fields. Resuspension is also studied using tracers and contaminated surfaces. The objective of the resuspension studies is to develop and verify models for predicting the airborne concentrations of contaminants over areas with surface contamination, development of resuspension rate predictors for downwind transport, and development of predictors for resuspendion input to the food chain. These models will be of particular relevance to the evaluation of deposition and resuspension of both radionuclides and chemical contaminants.

Transport of tracers and contaminants from the Geysers Geothermal Site is being evaluated using surface and aircraft sampling data. The ventilation of tracing a SF^6 tracer from Brush Creek Valley during sunrise is being evaluated by surface and aircraft sampling data.

• Atmospheric Diffusion in Complex Terrain

Objectives of this study are:

Defining and developing a long-range technical plan for studying the transport and diffusion of contaminant particles and gases over complex landforms.

Assisting a multilaboratory program studying diffusion in complex terrain by providing methodologies and techniques for analyses of transport and diffusion over a variety of complex landforms.

Evaluating and developing various transport and dispersion models for complex terrain.

THE TRANSPORT OF TRACERS AND POLLUTANTS FROM THE GEYSERS GEOTHERMAL RESOURCE AREA

M. M. Orgill, R. N. Lee and R. I. Schreck

The emission, transport, and dispersion of pollutants from energy production areas in complex landforms is a subject of continuing concern because emitted contaminants may cause a significant impact on the general public and environment through the mechanisms of chemical reaction, impaction, dry deposition and acid precipitation.

A limited surface and aircraft sampling study was conducted in the Geysers-Calistoga Geothermal Resource Area (GGRA) to collect initial data on the short-range (5 to 20 km) transport of contaminant materials and the short-range transport of a sulfur hexafluoride (SF_6) tracer from the geothermal electrical power generation area.

Pacific Northwest Laboratory (PNL) conducted the sampling study during the Department of Energy's (DOE) Atmospheric Studies in Complex Terrain (ASCOT) cooling tower field program as part of the daytime limited-mixing experiments (Gudiksen 1982). On August 23 and 24, the ASCOT group conducted extensive meteorological and tracer experiments during the daytime and evening hours. An SF_6 tracer was released from a power plant's cooling tower during the afternoon of each day. The SF_6 tracer was sampled by a surface network of samplers and by PNL and Meteorology Research, Inc. (MRI) aircraft. The PNL aircraft flew a flight track between 5 to 20 km upwind and downwind of the Geysers while the MRI aircraft flew closer to the source over the Mayacmas Ridge. In addition to these two days, the PNL aircraft also sampled for gaseous sulfur (H_2S) and airborne aerosols on August 20 and 21.

The goals of the PNL study were fourfold: 1) to define the types and quantities of airborne materials (e.g., H_2S, B, As, Cd, Pb, Cr, and Hg) that are emitted from the geothermal operations, 2) collect data on the location, height, and concentration of the airborne materials and SF_6 tracer, 3) examine the role of vertical wind shear in the transport of the H_2S and SF_6 tracer plumes, and 4) if possible, estimate the flux of pollutant material being transported from the Geysers.

The instrumentation, sampling procedures, weather conditions, and preliminary analysis of the data have been reported in PNL-4797 (Orgill, Lee and Schreck 1983). This report briefly discusses the results to date and outlines the future tasks necessary to complete the work. The final analysis and conclusions will be reported as an ASCOT report.

SF_6 Tracer Transport from the Geysers

On August 23 and 24, 1981, an SF_6 tracer was released from the cooling towers of Units 9 and 10, at a rate of 3 gm/s from 1300 PST to 1900 PST. Units 9 and 10 are located on a ridge southwest of Cobb Mountain at an altitude of 968 m above mean sea level. Because the analysis is not complete, only preliminary results from August 24 will be discussed. Table 1 outlines some of the variables considered important in the transport of the cooling tower plume and SF_6 on August 24. The meteorological conditions were complex and not easily understood, but were typical of many situations involving wind shear and time-varying wind conditions.

The wind and stability conditions were such that a portion of the cooling tower plume impacted at downwind surface locations. Figure 1 shows that a portion of the plume was observed at the surface throughout the

TABLE 1. Important Variables Affecting the Transport and Diffusion of SF_6 from Units 9 and 10, August 24, 1981

Variable	Comments
Plume rise	Average maximum plume rise around 1100 m or 2060 m m.s.l. (Uthe 1982)
Stability	SF_6 detected on the surface downwind from Units 9 and 10
Low-level wind speeds	Average wind speeds in a 350-m layer 3 to 5 m/s
Horizontal and vertical wind shear	Winds were backing and increasing in speed with height
Diurnal winds	Winds in lower elevations changed direction from west-southwest to west-northwest
Terrain influences	Possible gravity waves at higher elevations

Anderson-Putah Creek area and Boggs Mountain. The plume impaction occurred toward the northeast in the early afternoon and then shifted toward the southeast later in the afternoon. This change in direction of the surface impaction matches some wind observations that showed wind direction changing to more northwesterly directions after 1700 PST.

The principal plume axis at the three different aircraft sampling altitudes was oriented in generally the same direction as shown near the surface (i.e., toward the east and northeast). Maximum concentrations in the elevated plumes were above 200 parts per trillion (ppt). An increase in altitude shows a more diffuse plume with secondary maxima toward Middletown and east to northeast of Mt. Hannah (Figure 2). The apparent maximum concentration near Mt. Hannah at around 1600 m is of interest because of the high plume rise and upper vertical wind shear present during the sampling period. Another interesting feature was revealed by the SRI International airborne lidar. These measurements showed wavy undulations in the aerosol boundary layer at sampling altitudes (Uthe 1982). The presence of gravity waves may possibly account for the secondary SF_6 maximum just east of Mt. Hannah. However, these measurements and data from other aircraft passes will have to be investigated in more detail to determine if this provides a consistent description of the observed dispersion behavior.

Gaseous Sulfur (H_2S) Transport from The Geysers

One of the primary contaminants from the Geysers is gaseous sulfur in the form of H_2S, although other chemical forms can be present (e.g., SO_2). Surface and aircraft filter samples of particulates generally indicated sulfur (sulfate) enrichment above background levels in the collected aerosol. On the two days of SF_6 release from Units 9 and 10 (August 23 and 24), a minor amount of gaseous sulfur was contributed to the Geysers sulfur plume by SF_6. A low-concentration gaseous sulfur plume was detected on all four days in the eastern quadrants from the Geysers, because the winds were generally from southwesterly to westerly directions. The first estimates of H_2S concentrations as reported in Orgill, Lee and Schreck (1983) are suspected of being high by about 30%. A tentative correction was applied to the H_2S concentration data for PNL-4797, but these data will have to be further assessed in FY 84 to obtain the final concentrations and associated error limits.

Composition, Enrichment, and Transport of Geysers Aerosols

The four days of sampling resulted in 41 filters. Twenty-three filters (16 surface, 7 aircraft) were initially selected for x-ray fluorescence (XRF) and neutron activation analysis (NAA) (23 by XRF, 8 by NAA). Concentrations were obtained for 55 trace materials. In general, most of the trace materials had concentrations in the ng/m^3 range with the exception of iron (Fe) and sulfur (S), which were in the μg/m^3 range.

A crustal enrichment factor was computed for all 55 elements associated with the 23 filters. The crustal enrichment factor

$$EF_c = (C_x/C_{Fe})_{aerosol}/(C_x/C_{Fe})_{crust} \qquad (1)$$

expresses the relative enrichment of an element as compared to its abundance in the earth's crust. An EF_c less than 1 indicates depletion of an element, whereas a value greater than 1 indicates enrichment of a given element relative to its crustal abundance. Generally, an enrichment factor of 10 or more is considered significant with respect to anthropogenic input to the atmosphere.

Trace elements of particular interest because of their potential toxicity hazard and environmental contamination are

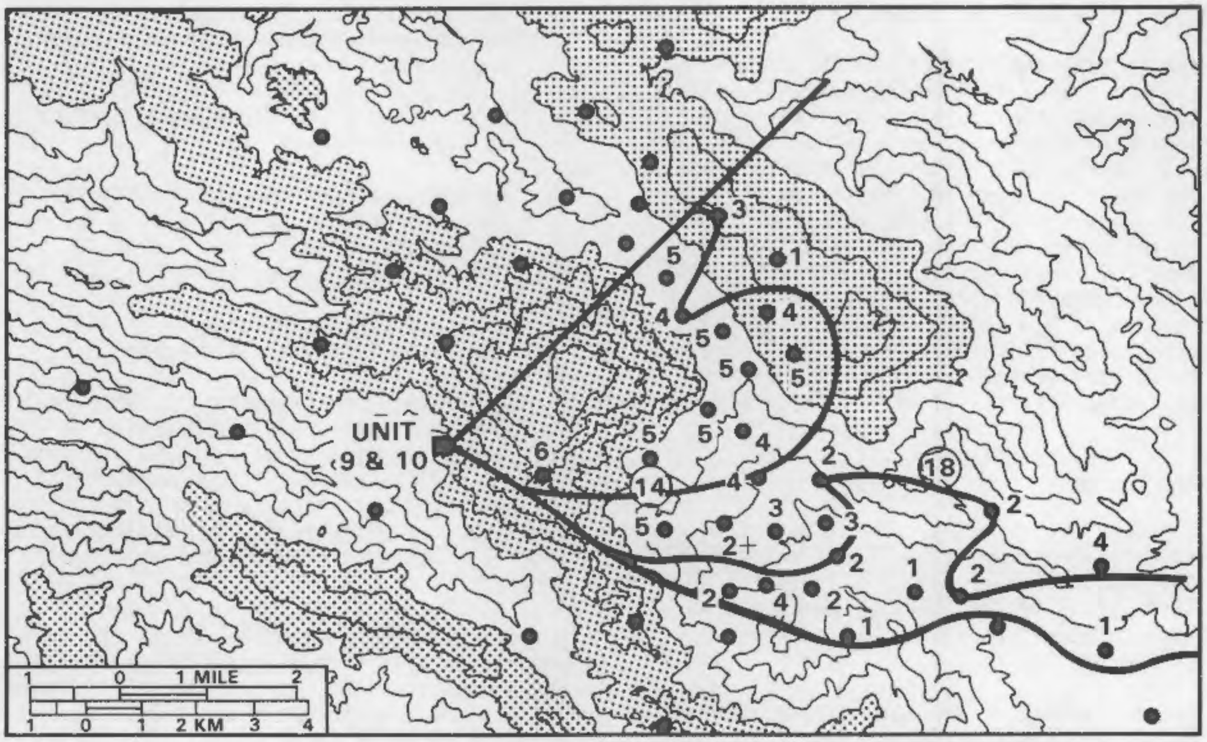

FIGURE 1. SF_6 Bag Sample Site Locations, Integrated Surface Plume Boundary, Plume Arrival Hours (14 and 18 PST) and Duration of Plume at Surface (hrs). Source: Units 9 and 10, August 24, 1981. Shaded Topography ≥ 853 m (2800 ft).

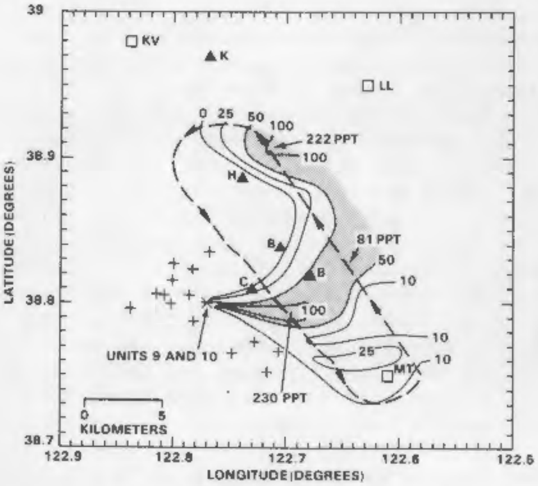

FIGURE 2. SF_6 Elevated Plume as Determined from Aircraft Samples of 5-second Average Concentrations, Elevation: 2580 m (5190 ft) m.s.l. Locations: Mt - Middletown , C - Cobb Mountain, H - Mt. Hannah, LL - Lower Lake, K - Mt. Kocnocti, KV - Kelseyville. Date: August 24, 1981.

sulfur (S), selenium (Se), boron (B), bromine (Br), lead (Pb), zinc (Zn), antimony (Sb), arsenic (As), barium (Ba), silver (Ag), cadmium (Cd), copper (Cu), manganese (Mn), fluorine (F) and mercury (Hg). To date, results show that several of these elements were significantly enriched above background levels within and downwind of the Geysers area at times. However, a number of sampling and analyses factors need to be considered in evaluating the data.

The analysis for trace elements is incomplete, and fourteen to seventeen additional filters need to be analyzed. Boron (B) a major element in geothermal steam and fluorine (F) have yet to be analyzed in any of the samples. The meteorological conditions during the sampling periods need to be examined and analyzed in order to determine the possible role of winds and temperature conditions during the sampling periods.

Other Data Analysis Tasks

The initial analysis of the SF_6 tracer transport data from the Geysers illustrates the effects that terrain, vertical wind, shear, time-varying winds and stability can have on the downwind distribution of cooling tower effluents during the daytime. These aspects of the transport problem will be evaluated in a more quantitative manner with the completed data analyses. In addition, the surface and aircraft sampling results of H_2S and trace materials, and meteorological parameters, particularly wind, will be used to estimate the flux of pollutant materials from the Geysers area.

References

Gudiksen, P. H. 1982. ASCOT Data from the 1981 Cooling Tower Plume Experiments in the Geysers Geothermal Area. UCID-19332, ASCOT-82-4, Vols. 1 and 2, Lawrence Livermore National Laboratory, Livermore, California.

Orgill, M. M., R. N. Lee and R. I. Schreck. 1983. Transport of Tracers and Pollutants from the Geysers Geothermal Resource Area. PNL-4797, Pacific Northwest Laboratory, Richland, Washington.

Orgill, M. M., R. N. Lee and R. I. Schreck. 1983. "The Transport of H_2S and Trace Materials from the Geysers Geothermal Resource Area." PNL-4600, PT3, In Pacific Northwest Laboratory Annual Report for 1982 to the DOE Office of Energy Research, Part 3 - Atmospheric Sciences, pp. 23-25, Pacific Northwest Laboratory, Richland, Washington.

Uthe, E. E. 1982. "Airborne Lidar Study of Plume Behavior in the Geysers Geothermal Area." In ASCOT Data from the 1981 Cooling Tower Plume Experiments in the Geysers Geothermal Area. UCID-19332, ASCOT-82-4, Vol. 2, pp. 8-58 to 8-59, Lawrence Livermore National Laboratory, Livermore, California.

THE VENTILATION OF AN SF_6 TRACER FROM A MOUNTAIN VALLEY

M. M. Orgill, R. N. Lee and R. I. Schreck

An important component of the joint EPA-DOE (GRAMA-ASCOT) field experiment in Brush Creek, Colorado, in July-August 1982 was an aircraft SF_6 sampling task. The objectives of this part of the experiment were

1. to provide data on the location, height, and concentration of SF_6 over Brush-Roan Creek Valleys,
2. to supplement the Brush Creek surface sampling network,
3. to evaluate the fumigation and ventilation of the SF_6 tracer in the valley and assist in evaluating the GRAMA computer valley model (VALMET), and
4. to assist the ASCOT program in the design of future field programs.

The experiments, instrumentation, and preliminary sampling results were presented last year in Orgill et al. (1983). In this report, preliminary results of analyzing the real-time aircraft SF_6 data will be presented. Final results of the aircraft sampling task will be published at a later date.

Composites were constructed of the SF_6 concentration data from aircraft observations, the Sandia profiler, and surface-slope sampling sites from the July 31, August 4, and August 6 data for two periods. The first period encompassed the time period that wind was down-valley. The second period included the transition period (sunrise) and the initiation of the up-valley wind.

The SF_6 plume during the drainage wind period was observed to be confined below 300 m in the valley. Figure 1 shows the composite plume configuration and SF_6 concentration during the up-valley wind transition. The plume is entrapped, for the most part, in the valley except where the Sandia profiler and aircraft observations show the plume diffusing to higher levels and toward the sunny west-sidewall. Concentrations were above 100 parts per trillion (ppt) on the sunny west-sidewall and near the summit of Brush Mountain. Concentrations over Skinner Ridge were near background. During the later part of the up-valley wind period, concentrations above 200 ppt were detected over and up-valley of the release site and also over Brush Mountain and Skinner Ridge.

The data on the 5-second SF_6 concentrations from aircraft samples for the period between 0748 and 0825 MST August 6 are shown in Figure 2. Higher concentrations of SF_6 were detected over Brush Mountain and the Brush Creek Valley west-sidewall and lower concentrations were detected over Skinner Ridge.

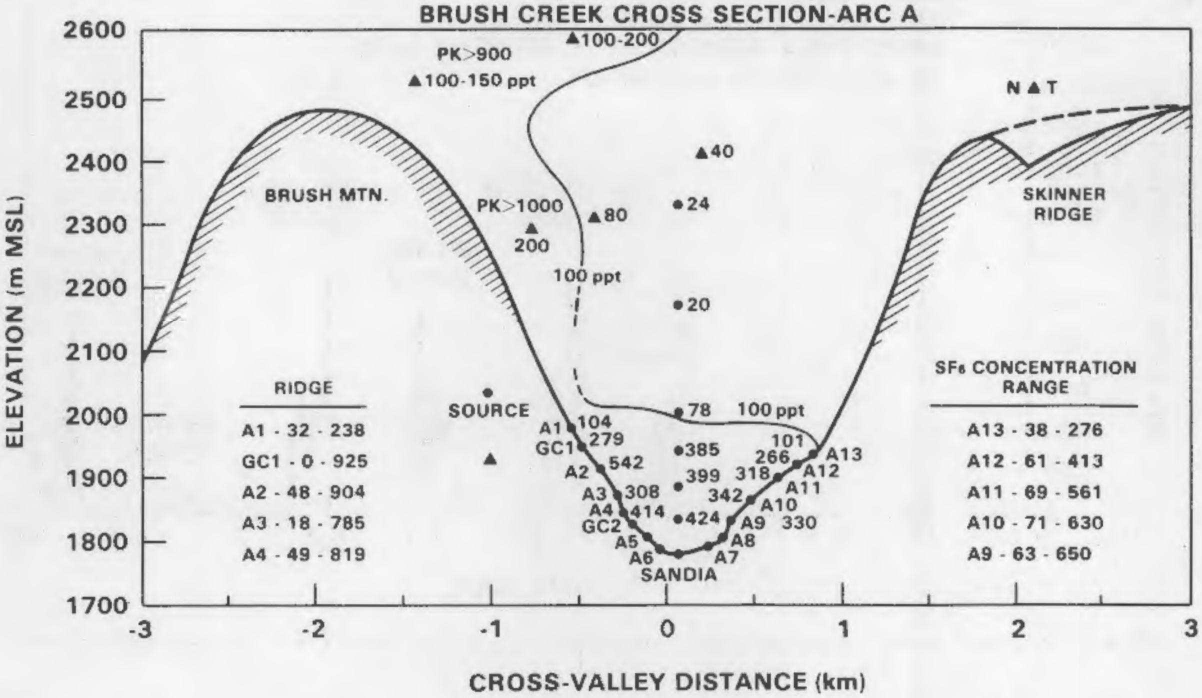

FIGURE 1. SF_6 Concentration Data from Aircraft, Sandia Profiles, and Slope Stations for July 31, August 4 and August 6, 1982 (Up-Valley Winds).

An examination of all aircraft SF_6 sampling data and the surface-sampling data provided important information on the ventilation of tracers and pollutants from a valley. Some tentative conclusions follow.

1. A release rate of 8 or more kg/hr of SF_6 provides measurable concentrations at higher elevations of the valley.
2. The SF_6 plume was carried by drainage winds out of Brush Creek and down Roan Creek to 20 km or more.
3. Concentrations in excess of 100 ppt were observed near the west-sidewall of the valley and over Brush Mountain after two hours past sunrise.
4. Little tracer was detected over the east ridge near the mouth of Brush Creek even after sunrise.
5. The SF_6 plume moved to the west-sidewall after sunrise and was ventilated up the valley wall to ridge levels. This observation is consistent with the hypothesis of upslope and up-valley transport of tracer in a developing convective boundary layer in the valley.

Reference

Orgill, M. M., C. D. Whiteman, R. N. Lee and T. R. Heimbigner. 1983. "Temperature Inversion Breakup in Mountain Valleys and the Ventilation of Pollutants - The Joint GRAMA-ASCOT Field Experiment 1982." PNL-4600, PT3, In Pacific Northwest Laboratory Annual Report for 1982, Part 3, Atmospheric Sciences, Pacific Northwest Laboratory, Richland, Washington.

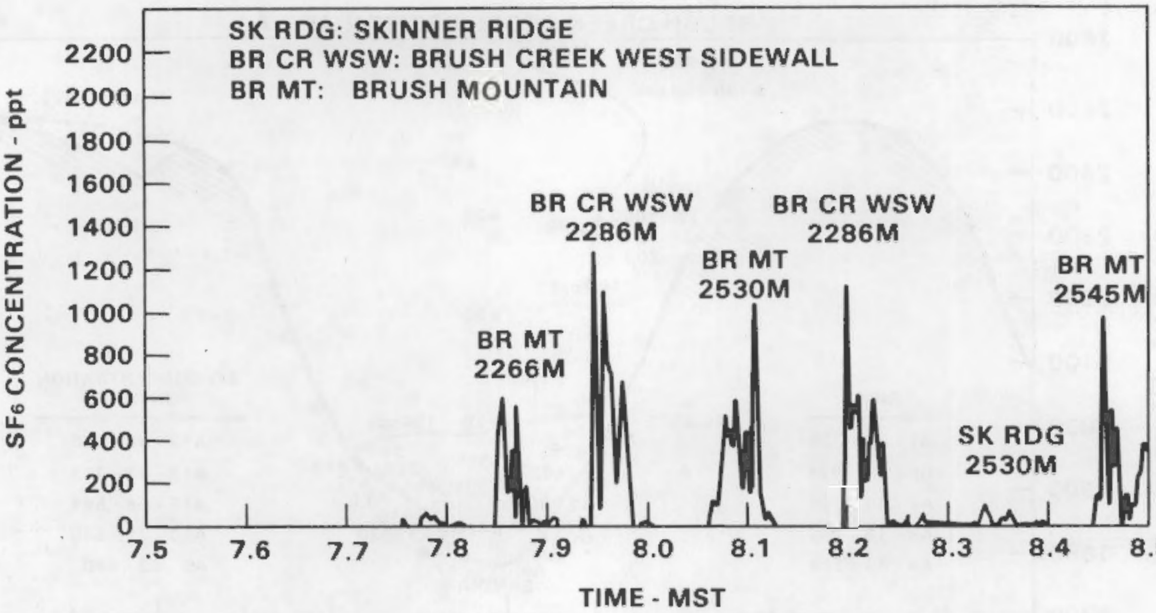

FIGURE 2. Average 5-Second Concentration of SF_6 from Aircraft Sampling over Brush Creek, Colorado, August 6, 1982.

• Atmospheric Boundary Layer Studies

Objectives of these studies are:

Investigating the meteorological characteristics of the planetary boundary layer that pertain to pollutant transport and dry removal.

Analyzing the transport and diffusion of contaminants in complex terrain, particularly in the Geysers Geothermal Area of California.

Constructing simple models for predicting the depth, speed and direction of gravity-controlled drainage flows and contaminant dispersion within these flows.

ESTIMATES FOR PESTICIDE PROFILES ABOVE TREATED FIELDS

T. W. Horst and W. G. N. Slinn

Glotfelty et al. (1983) have reported concentration profiles for pesticides above a treated field (Figure 1a). In their report they suggest that differences in the normalized profiles (Figure 1b) were caused by influences on turbulent diffusion from different molecular diffusivities of the pesticides. Since this inference conflicts with common practice and may have important implications for the diffusion of airborne contaminants, it is important to examine the data carefully and, as appropriate, search for alternative interpretations. Horst and Slinn have found that the differences in the profiles are more likely

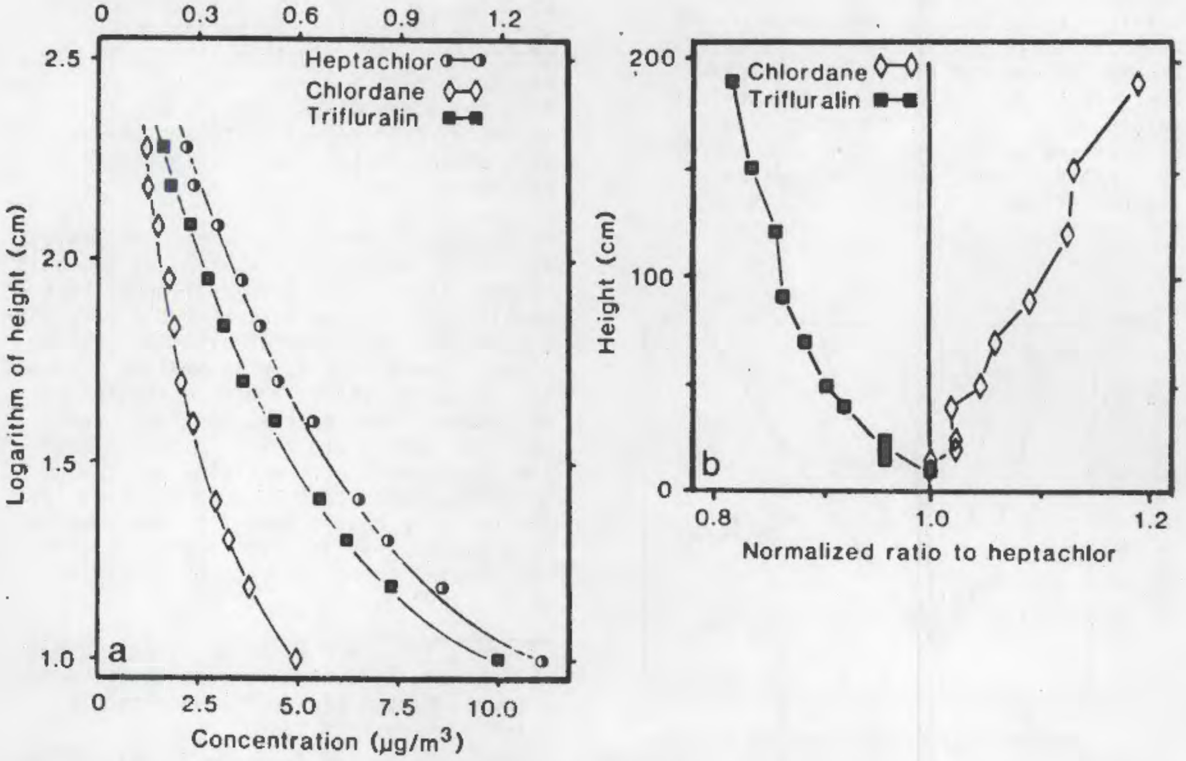

FIGURE 1. Concentration Profiles (a) and Concentration Ratios (b) Reported by Glotfelty et al. (1983). The ratios were normalized to the value unity at z = 10 cm.

caused by different, fetch-dependent surface-to-air fluxes of the pesticides.* These, in turn, are dictated by different air/surface partition coefficients for the different pesticides.

Our response to Glotfelty et al. was based on solutions of the convection-diffusion equation describing downwind advection and vertical diffusion of pollutants suspended from a surface area source. The surface-to-air pesticide flux was determined by a simple film model and was found to be proportional to the difference between the pesticide concentration in air at the soil surface and the airborne pesticide concentration that would be in equilibrium with the bulk concentration in the soil. The proportionality factor k_o is an effective transfer velocity, which is a function of the air/surface partition coefficient H and the transfer velocities through the surface film (k_s) and through the air's viscous sublayer (k_a),

$$k_o^{-1} = H\, k_s^{-1} + k_a^{-1}.$$

Pesticide profiles were predicted analytically for the case of wind speed U_o and eddy diffusivity K_o independent of height. Figure 2 shows the resulting pesticide concentration-ratio profiles for several values of $p = k_o/U_o$. Comparing Figure 2 with Figure 1b suggests that this approach is capable of describing the dominant feature of the data and that it is unnecessary to assume that diffusion in a turbulent atmosphere is influenced by molecular properties of the dispersing vapor.

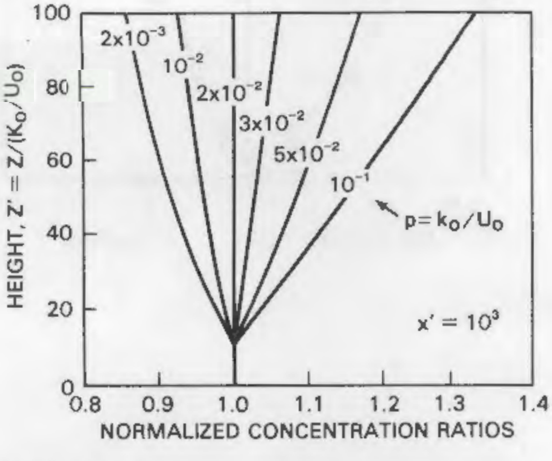

FIGURE 2. Concentration Ratios Obtained from the Analytical Solution with Constant Wind Speed, Uo, and Eddy Diffusivity, Ko.

In the interpretation presented by Horst and Slinn, differences in normalized profiles for different pesticides are a direct consequence of the dependence of the surface-to-air flux on the local, airborne concentration of pesticide. Without this dependence and if the pesticide concentrations were spatially uniform in the soil, then the flux of each pesticide would not depend on location, and the normalized pesticide profiles would be identical. On the other hand, with this dependence, the fluxes decrease with distance from the upwind edge of the field, at a rate that is different for each pesticide because of the differences in transfer velocities caused by the different values of H.

Pesticide profiles have also been predicted numerically for the more realistic case where wind speed and eddy diffusivity are a function of height, using the surface flux model of Horst (1978). In this analysis Horst and Slinn** suggest that the height-to-fetch ratio for the data may not have been the 100 to 1 ratio suggested by Glotfelty et al. Instead, it may be that as the pesticide evaporated (preferentially from the edges of the field), the height-to-fetch ratio decreased to smaller values, such as the 10 to 1 ratio illustrated in Figure 2.

Horst and Slinn** also comment upon values for the parameters k_s, k_a, and H. In this regard, they note the rule-of-thumb that usually the more complex the molecule, the smaller its air/surface partition coefficient. Consequently, with smaller H values and larger k_o values for more complex molecules, their evaporation rates would decrease more rapidly with distance from the upwind edge of the field, and their airborne concentration would decrease less rapidly with height than for less complex molecules. This is also consistent with the general trend reported by Glotfelty et al. (1983).

---

*Horst, T. W. and W. G. N. Slinn. 1983a. "Atmospheric Concentrations of Pesticides Above Treated Fields." Submitted for publication in Science.

**Horst, T. W. and W. G. N. Slinn. 1983b. "Estimates for Pollution Profiles Above Finite Area-Sources." Submitted for publication in Atmos. Env.

References

Glotfelty, D. E., A. W. Taylor and W. H. Zoller. 1983. "Atmospheric Dispersion of Vapors: Are Molecular Properties Unimportant?" Science 219:843-845.

Horst, T. W. 1978. "Estimation of Air Concentrations Due to the Suspension of Surface Contamination." Atmos. Env. 12:797-802.

EVALUATION OF THE MODIFIED SOURCE-DEPLETION MODEL

T. W. Horst

The airborne contamination resulting from a point source release is most commonly estimated with the Gaussian plume dispersion model. Because estimates of the plume dimensions are empirical, model predictions can be fairly realistic in many situations. Ideally, these plume dimensions are measured with passive, nonreacting, nondepositing tracers so that they only reflect the dispersion process. Hence, application of the Gaussian model for a depositing pollutant requires that it be modified to account for the reduced airborne concentrations and to estimate the resulting surface contamination. Because it does not explicitly treat the vertical transport process, the diffusion model is difficult to modify in a way that is physically realistic.

Horst (1977) showed that the common source-depletion technique used to account for the loss of material from a Gaussian plume, overestimates the near-surface airborne concentration and the dry deposition because the model distributes the loss resulting from dry deposition throughout the vertical extent of the plume and retains the Gaussian vertical concentration profile. Horst (1980) proposed a correction to the source-depletion model that accounts for the change in the vertical concentration profile caused by deposition. This correction to the vertical distribution is a function of the resistance of the atmosphere to vertical turbulent transport and is derived using gradient-transport theory. During the past year, the theoretical foundation of this correction has been developed further and additional comparisons have been made with the surface-depletion model (Horst 1983).

Without deposition, the Gaussian plume model predicts the airborne pollutant concentration Co to be

$$Co(x,y,z) = Qo\ D(x,y,z,h) \qquad (1)$$

where Qo is the rate of pollutant emission and $D(x,y,z)$ is the Gaussian diffusion function for a point source located at $(x=0,y=0,z=h)$. The corrected source-depletion model,

$$Cd(x,z) = Q(x)\ D(x,y,z,h)\ P(x,z) \qquad (2)$$

makes two modifications to the Gaussian plume model. The source strength $Q(x)$ is reduced with downwind distance to account for the loss of material from the plume by dry deposition, and the Gaussian distribution D is modified by the profile function, $P(x,z)$, to account for the change in the vertical distribution caused by removal of material at the surface. Conservation of mass requires that

$$Q(x) = Qo\ \exp\left[-\int_{-\infty}^{\infty}\int_{0}^{x} v_d\ D(x',y',z_d,h)\ P(x',z_d)\ dx'\ dy'\right] \qquad (3)$$

where z_d is the height at which the deposition velocity v_d is defined. With $P=1$, Equations (2) and (3) reduce to the usual source-depletion model.

With a minimum of assumptions, the near-surface profile function, $P(x,z)$, can be related to the atmospheric resistance to vertical transport (Horst 1980, 1983). However, the atmospheric resistance, $R(z,z_d)$, is a function of the eddy diffusivity, which depends on height, while the vertical spread of a Gaussian plume is expressed in terms of a diffusion coefficient, σ_z, which depends on downwind distance. Unfortunately, as a consequence, the appropriate atmospheric resistance for a Gaussian plume is determined only by a nonrigorous, heuristic argument relating the diffusion coefficient to the eddy diffusivity. The validity of this argument must be judged by the quality of the resulting predictions.

The corrected source-depletion model can be tested by comparing its predictions either with observations or with the predictions of a more rigorous model. Few observations of plume depletion are available, but the surface-depletion model (Horst 1977) is an exact modification of the Gaussian plume model to account for deposition. It is ideal for evaluating the corrected source-depletion model because the two models differ only in their description of plume depletion. They have the same input and the same assumptions about the diffusion process.

The two models agree well for predictions of suspension ratios and for predictions of depleted airborne concentrations near the surface (Horst 1980, 1983). These two quantities have a high practical significance, but they are indirect functions of the atmospheric resistance. A more direct test of the predicted atmospheric resistance is a comparison of the vertical airborne pollutant concentration profiles predicted by the two models. Such a comparison is shown in Figure 1 for a situation with relatively high deposition: a source height of 10 m and stable atmospheric conditions. Since $\partial P/\partial z = P(x,z_d)\ v_d\ \partial R/\partial z$, the excellent agreement of the two models below $z=\sigma_z$ validates the expression for the atmospheric resistance as a function of the Gaussian vertical diffusion coefficient. The relatively poorer agreement above $z=\sigma_z$ is expected because the profile function is only valid in a layer near the surface where, without deposition, the airborne concentration is independent of height.

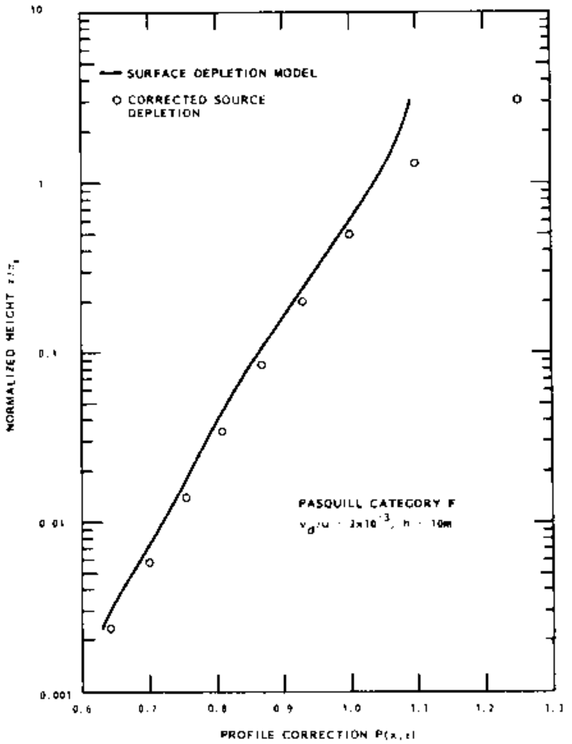

FIGURE 1. The Profile Correction as a Function of Height at 2 km Downwind of the Source.

References

Horst, T. W. 1977. "A Surface Depletion Model for Deposition From a Gaussian Plume." Atmos. Environ. 11:41-46.

Horst, T. W. 1980. "A Review of Gaussian Diffusion-Deposition Models." In Atmospheric Sulfur Deposition, Environmental Impact and Health Effects, D. S. Shriner, C. R. Richmond, and S. E. Lindberg, eds., Ann Arbor Science, Ann Arbor, Michigan.

Horst, T. W. 1983. "A Correction to the Gaussian Source Depletion Model." In Precipitation Scavenging, Dry Deposition and Resuspension, H. R. Pruppacher, R. G. Semonin and W. G. N. Slinn, eds., Elsevier Science Publishers, Amsterdam, The Netherlands.

• Dry Deposition

Objectives of this study are:

Developing an experimental basis for models predicting removal of airborne particles and gases by dry deposition onto outdoor surfaces.

Developing predictive models accounting for the influence of particle size, gas characteristics, wind velocity, deposition surface, and other variables on deposition rates.

Determining deposition rates using dual tracer techniques in the field and in a wind tunnel in the laboratory.

IMPROVED PREDICTIONS OF DRY-DEPOSITION VELOCITY OF PARTICLES

G. A. Sehmel

A correlation was developed by Sehmel and Hodgson (1980) for predicting particle dry-deposition velocities. Deposition velocity is defined as the deposition flux (units of amount deposited per unit ground-surface area per unit time) divided by the airborne concentration at a selected height above the ground (amount per unit volume), and is usually reported in units of cm/s. The correlation was based upon deposition velocities evaluated in wind tunnel experiments for non-living surfaces of different aerodynamic surface roughness. A weighted least-squares technique was used to correlate the logarithm of mass-transfer resistances in terms of the logarithms of dimensionless groups and particle diameter. The dimensionless groups are the Schmidt number (ν/D), the particle relaxation time (τ^+), a ratio of Brownian to eddy diffusivity (D/z_0u_*), and a length ratio (d/z_0). The multiple correlation coefficient was 0.92 and all coefficients were statistically significant at the 99% level.

Subsequently, deposition velocities were predicted as a function of particle diameter from 0.03 to over 50 μm. However, the correlation was inadequate for predictions below 0.03 μm diameter. That is, rather than increasing, predicted deposition velocities started to decrease as particle diameter was decreased below 0.03 μm.

The correlation was used to predict particle dry deposition velocities for a height of 1 m. This height is often used for a boundary condition over surfaces without large vegetative canopies in meteorological transport and diffusion models. The modeling approach was to combine mass-transfer resistances in the 1 cm adjacent to the surface determined by the correlation, with aerodynamic mass transfer resistances from 1 cm to 1 m determined by the diffusivity equations of Businger et al. (1971). The correlation was further developed to predict the surface mass-transfer resistance (reciprocal deposition velocity) in the lower 1 cm adjacent to uniform deposition surfaces without deep vegetative canopies. In this case, the objective was to develop a mass transfer resistance predictor that could be used as a boundary condition for meteorological transport and diffusion models in which aerodynamic resistances were described for heights closer than 1 m to the deposition surface.

When the correlation was developed, particle diffusivities were assumed equal to air-momentum diffusivities. However, the validity of this assumption is dependent on the relative mass transfer resistances at and above the deposition surface. Currently, the equality to heat diffusivity is often considered more appropriate. Nevertheless, the diffusivity selection may be a second order effect. In practice, the use of either momentum or heat diffusivity is only of secondary importance for predicting deposition velocities for particle diameters ranging from about 0.1 to 1 μm. For these diameters, deposition velocities are controlled by surface resistances in the 1 cm adjacent to surfaces of low relief. In addition, selecting the proper diffusivity may be of minor importance compared to the uncertainties in predicting integrated surface resistances as a function of height and spatial variation in vegetative canopies.

Dry-deposition velocities are complex functions of the parameters determined. The correlation predicts dry deposition velocities as a function of particle diameter, friction velocity and aerodynamic surface roughness. Also, since the experimental particle density was 1.5 g/cm^3, the influence of particle density is predicted by including particle settling velocities in the prediction equations.

Because predictions are complex functions of these variables, researchers have approximated predicted deposition velocity curves. However, these simplifications may be compounding prediction uncertainties, because uncertainties exist in the original correlation.

Hence, particle dry-deposition velocities evaluated with monodispersed-diameter particles in wind tunnel experiments were re-examined using least squares techniques to develop an improved predictive correlation.

Correlation

Least-squares techniques were used to correlate either the deposition velocity, or integral resistances, as used in the original correlation, as a function of both particle diameter and dimensionless groupings. Logarithmic transformations were used in the least squares analyses. Many correlations were examined for the highest multiple correlation coefficient. This examination included the evaluations of the statistical significance of the first through third powers of each dimensionless group examined, and interactions between groups. Third powers were statistically insignificant. The final correlation predicts deposition velocities, $K_{1\text{-cm}}$ with an airborne concentration at 1 cm (which has the highest multiple correlation, and is without variables that are highly correlated with other predictor variables). The multiple correlation coefficient is 0.95 (versus 0.92 in the 1980 correlation) and all coefficients are statistically significant at the 99% level. The final correlation relates the logarithm of deposition velocity as a function of the logarithms of dimensionless groups and particle diameter. Particle diameter is expressed in centimeters. The dimensionless groups are the Schmidt number (ν/D), the particle relaxation time (τ^+), a ratio of Brownian to eddy diffusivity (D/z_0u_*), and a length ratio (d/z_0). The correlation of deposition velocities as an exponential function of the logarithms of dimensionless groups and particle diameter follows:

$$K_{1\text{-cm}} = \exp\Big\{7.108 + [\ln(Sc)\ \ln(d/z_0)][0.2529 - 0.00273\ \ln(d/z_0)] + [\ln(\tau^+)][0.03239\ \ln(\tau^+) - 0.09177\ \ln(d/z_0)] - 0.14919\ [\ln(d)]^2 - 4.180\ \ln(d/z_0)\Big\} \quad . \tag{1}$$

where

a = particle radius, cm
d = particle diameter, cm
D = Brownian diffusion coefficient sq. cm/sec (see Equation 2)
k = Boltzmann's constant, 1.38×10^{-16} erg/(molecule °K)
p = pressure, cm of mercury (76.0 cm used)
Sc = Schmidt number, ν/D
T = temperature, °K (296°K used)
u_* = friction velocity, cm/sec
z_0 = aerodynamic surface roughness, cm
μ = air viscosity, g/(cm·sec) [1.78×10^{-4} g/(cm·sec) used]
ν = kinematic viscosity, μ/ρ
ρ = air density, g/cc, (1.2×10^{-3} g/cc used)
$\tau+$ = dimensionless relaxation time,

$$\frac{\rho_p d^2}{18\mu}\ \frac{u_*^2}{\nu}$$

The Brownian diffusivity was calculated from (Davies 1966):

$$D = \frac{kT}{6\pi\mu a}\Big\{1 + \frac{10^{-4}}{pa}\ [6.32 + 2.01\ \exp(-2190pa)]\Big\} \tag{2}$$

Ratios of predicted/experimental deposition velocities were evaluated as indices for agreement between predicted and experimental results. The average ratio is 1.46, the maximum ratio is 19.3, the minimum ratio is 0.82, and the standard deviation is 1.78.

Also, ratios of predicted deposition velocities between the correlation developed in 1980 and Equation 1 were evaluated to show agreement between the two correlations for the experimental conditions investigated (i.e., the ratio K_{1980}/K_{1983}). In this case, the average ratio is 1.13, the maximum ratio is 3.88, the minimum ratio is 0.44, and the standard deviation is 0.68.

Predictions for Constant Friction Velocity

Predicted deposition velocities for a 1-cm concentration reference height, K_1-cm, from the 1980 and 1983 correlations are compared in Figure 1 as a function of aerodynamic surface roughness for a constant friction velocity of 30 cm/s and particle density of 1.5 g/cm^3. Also shown are gravitational settling velocities for spherical particles. The following features are emphasized.

- Predictions from the 1983 correlation (as opposed to predictions from the 1980 correlation which have a lower particle diameter limit of 0.03 µm) show trends expected for particle diameters as small as 10^{-2} µm (i.e., deposition velocities continue to increase as particle diameter decreases below the particle diameter for minimum dry-deposition velocity).
- Minimum deposition velocities are functions of the aerodynamic surface roughness.

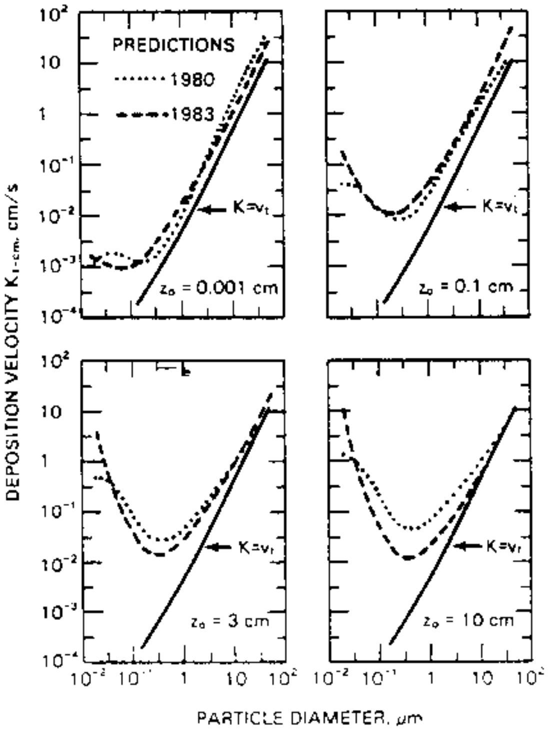

FIGURE 1. Particle Size Distributions for Uranine and Lithium Carbonate Tracers.

- Dry-deposition velocities are greater than gravitational settling velocities.
- Aerodynamic resistances from 1 cm to 1 m are increasingly important for large particles. Predicted deposition velocities for a 1-m concentration reference height would be similar to gravitational settling velocities. In comparison, because aerodynamic resistance is not included, deposition velocities for a 1-cm concentration reference height can be significantly greater than gravitational settling velocities for particle diameters as large as 50 µm.

Conclusions

An improved correlation was developed for predicting particle dry-deposition velocities. Improvements included an extension in the range of applicability to particle diameters as small as 10^{-2} µm, and an increased multiple correlation coefficient to 0.95. Nevertheless, needed predictive improvements include methods to predict effects of deeper canopies, vegetative canopies, nonuniform canopies, nonspherical particles, and simultaneous resuspension for particles of 10 to 20 µm diameter.

References

Businger, J. A., J. C. Wyngaard, Y. Izumi and E. F. Bradley. 1971. "Flux-Profile Relationships in the Atmospheric Surface Layer." J. Atmos. Sci. 28:181-189.

Davies, C. N. 1966. Aerosol Science. Academic Press, New York.

Sehmel, G. A. and W. H. Hodgson. 1980. "A Model for Predicting Dry Deposition of Particles and Gases to Environmental Surfaces." In Implications of the Clean Air Act Amendments of 1977 and Energy Considerations for Air Pollution Control. Symposium Series No. 196, No. 76, pp. 218-230. American Institute of Chemical Engineers, New York.

DRY DEPOSITION EXPERIMENTS USING MULTIPLE TRACERS ON THE HANFORD DIFFUSION GRID

G. A. Sehmel

Experiments to measure dry deposition of particles were conducted for the Department of Energy (DOE) simultaneously with similar experiments sponsored by the Environmental Protection Agency (EPA). In the EPA experiments, zinc sulfide particles and SF_6 tracer gas were released. In the DOE experiments, two different tracers were released to determine dry deposition as a function of particle diameter. The tracers used were uranine and Li_2CO_3.

Particle dry deposition will be calculated from tracer particle/gas concentration ratios. The objective here was to investigate dry deposition for two nearly monodisperse tracer particles:

1. the diameter of Li_2CO_3 particles was about 1 μm (a diameter at which dry deposition velocities are minimum and nearly independent of particle diameter)
2. the diameter of uranine particles was significantly larger than 1 μm diameter.

Experimental Procedures

Particle size was strictly controlled in the experiments. Both tracers were generated in the field by using modified commercial paint sprayers. One paint sprayer was used for each tracer. The paint sprayer had the same general features as a spinning-disc aerosol generator used in the laboratory to generate monodispersed aerosol particles. The feed solution and operating parameters were different for each tracer.

Particle diameters were evaluated using quartz-crystal micro-balance cascade impactors. The mass median particle diameters were 17 μm for the uranine particles and 1.6 μm for the Li_2CO_3 particles (Figure 1). Densities of the tracer particles were 1.5 and 2.1 g/cm^3 for uranine and Li_2CO_3, respectively.

Tracers were released during drainage flows at the diffusion grid on the Hanford Site for several nights. The tracer release height each night was either 2.1 or 2.3 m above the ground. The average time that the tracer was released was 30 minutes. The average amounts of tracer dissolved in ethanol-water released were 17 g of uranine and 0.1 g of lithium as Li_2CO_3.

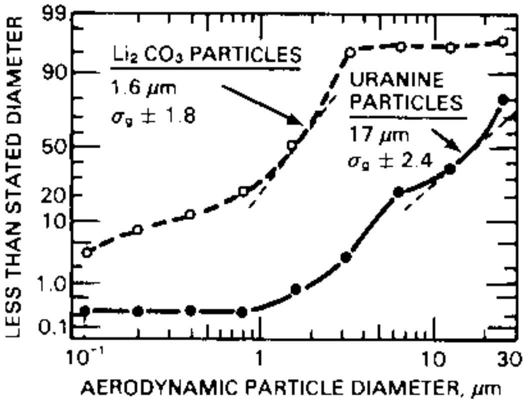

FIGURE 1. Particle Size Distributions for Uranine and Lithium Carbonate Tracers

After release, particulate tracers and tracer gas were collected as a function of crosswind direction along arcs at distances of 100, 200, 800, 1600, and 3200 m from the release site for the sector of the arc from 68° to 160° (0° = north). Spacing between samplers was 2° for the 100 and 200 m arcs, and 1° for the outer three arcs. Samples were collected at a height of 1.5 m.

Particulate tracers were collected on filters that are being analyzed for uranine and lithium content. To prepare the samples for analysis, tracers were leached from collection filters using 7 ml of water. Wash solutions have been analyzed fluorimetrically for uranine content, and subsequently, selected samples will be analyzed for lithium content.

Conclusions

Samples are being analyzed for tracer particle content for six nights. Results to date show that tracer plumes passed through the collection grid. However, plume characteristics varied from a well-captured plume within the sampling grid, to a plume with a bimodal crosswind distribution. Expected results will include dry deposition velocities for all six experiments for the uranine tracer particles. Although concentrations for the Li_2CO_3 particles were often lower than detection limits for ICP (induction coupled plasma) analyses, expected results include dry deposition velocities for Li_2CO_3 particles for distances between 100 and 200 m.

GENERATION OF NEARLY MONODISPERSED PARTICLES FOR DRY DEPOSITION FIELD EXPERIMENTS

G. A. Sehmel and W. H. Hodgson

Improved experimental techniques are needed to evaluate dry deposition of contaminants in the field. One needed improvement is a technique for generating large quantities of monodispersed tracer particles. A technique for generating tracer particles that was developed by Sehmel and Hodgson in 1980 was further developed. This technique will be used in field experiments to determine removal rates of particles by dry deposition as a function of diameter. The technique is based upon using a modified commercial paint sprayer that has the same general features of a spinning disc aerosol generator used in the laboratory to generate monodispersed diameter particles. Liquid droplets are formed along the edge of a rotating bell.

The objective was to establish the operating parameters for the particle generator that could be used during dry deposition field experiments beginning in May 1983. Design conditions included the following.

1. The two tracers should have different chemical compositions but be relatively inexpensive to analyze.
2. Tracer particles would approach a monodisperse size distribution.
3. Particle generation rates would be maximized.
4. The diameter of one tracer would be about 1 μm, a diameter at which dry deposition velocities are minimum and nearly independent of particle diameter.
5. The diameter of the second tracer would simulate diameters of fugitive emissions with the constraint that the particle size would be representative of particles that could be inhaled.

Experimental Procedures

Operating parameters for the field tracer-particle generator* were determined in the laboratory by evaluating particle diameter characteristics with a quartz-crystal microbalance (QCM)** particle cascade impactor. For each of the ten impactor stages, the manufacturers stated that 50% stage-collection efficiencies are 0.05, 0.1, 0.2, 0.4, 0.8, 1.6, 3.2, 6.4, 12.5, and 25 μm.

To evaluate tracer diameters as a function of operating parameters, tracers were generated within a wind tunnel, allowed to evaporate, and then were sampled with the QCM. After each evaluation, the wind tunnel was flushed with clean air before tracers were again introduced into the tunnel.

Operating parameters included bell rotation speed, liquid flow rates for constant liquid composition, and uranine solution concentration. Rotation speeds ranged from 5,000 to 38,000 revolutions per min (rpm), liquid flow rates ranged from 0.25 mℓ/min to 1.2 ℓ/min, and uranine concentration ranged from 0.25 to 140 g/ℓ.

Tracers in ethanol-water solutions were introduced at constant flow rates into the particle generator. The ethanol was used to increase evaporation rates. The particle diameter generated with each tracer was selected based upon uranine and Li_2CO_3 solubilities. Uranine was used for the larger particles because uranine solubility is over 140 g/ℓ, and lithium carbonate (Li_2CO_3) was used for the smaller particles because its solubility is much lower. Lithium carbonate solubility was estimated by dissolving Li_2CO_3 into different volume percentages (v/o) of ethanol and water. Results indicate Li_2CO_3 solubility is less than one gram per liter of 50 v/o ethanol, and greater than one gram per liter in 40 v/o ethanol. Consequently, lithium-traced particles were generated from a solution of 1 g/ℓ Li_2CO_3 in 40 v/o ethanol. Uranine particles were generated from a 20 g/ℓ solution of 80 v/o ethanol.

After determining what the operating parameters were, operating conditions selected for field tests are summarized in Table 1. Aerodynamic particle size distributions for both tracers are shown in Figure 1. Both size distributions approximate log-normal distributions, except that the distributions were truncated by preferentially removing either the smallest or largest diameter particles

---

* Model RAB-500, Rotary Atomizer, The DeVilbiss Company, Toledo, Ohio 43692.

** Model PC-2 QCM Cascade Impactor, California Measurements Incorporated, Sierra Madre, California.

TABLE 1 Particle Generator Operating Conditions Used for Field Experiments

Operating Conditions	Particles	
	Uranine	Li_2CO_3
Ethanol-water solution v/o ethanol	80	40
Tracer concentration, g/ℓ	20	1
Tracer flow rate, mℓ/min	31	23
Bell rotation speed, rpm	17,500	38,000
Satellite particle removal air flow rate, cfm	7.3	0
Particle removal impaction cylinder around rotating bell	Not used for this particle size	28-cm dia. cylinder, extending 30 cm in front and 15 cm in back of bell

during particle generation. For the log-normal portion of the size distribution, the mass median particle diameters are 1.6 µm for Li_2CO_3 and 17 µm for uranine, and the geometric standard deviations (σ_g) are approximately 1.8 and 2.4, respectively.

Conclusions

Operating conditions were determined for generating tracer particles of two different diameters. Better conditions may exist, but these results were satisfactory considering the time constraints imposed for initiating field experiments.

Reference

Sehmel, G. A. and W. H. Hodgson. 1983. "Development of a Near-Monodispersed Particle Generator for Field Dry Deposition Experiments." In Pacific Northwest Laboratory Annual Report for 1982 to the DOE Office of Energy Research, Part 3 Atmospheric Sciences, PNL-4600-3, pp. 34-36, Pacific Northwest Laboratory, Richland, WA.

• Particle Resuspension and Translocation

Objectives of this study are:

Investigating particle resuspension rates and air concentrations as functions of atmospheric stresses, local soil-working stresses, particle variables, surface variables, and deposit age.

Developing an experimental resuspension data base to aid in establishing surface contamination limits to assure adequate public protection from hazardous materials.

Factoring time-varying resuspension rates into models describing delivery of surface contaminants to man.

SPREAD OF TRACER FROM A RESUSPENSION SOURCE AREA OVER TIME

G. A. Sehmel

Contamination on the ground surface can be resuspended and become a hazard to man and to the environment. Resuspended contaminants can be deposited on edible portions of plants and introduced into the food chain. Models to evaluate resuspension and deposition rates to the plant surface are needed to determine these potential hazards.

Resuspensions of surface contamination by wind has been simulated using inert tracer sources on the ground (Sehmel 1983a). Through subsequent investigations, resuspension rates were found to increase with increasing wind speed, and resuspension rates were found to be nearly independent of time for several years.

In these experiments to determine resuspension rates, the airborne tracer was sampled as a function of height above the tracer source area. The resuspension rates were then calculated from a mass balance using integrated concentrations (airborne versus source concentrations). In these calculations, the concentration of tracer source (amount per unit ground area) was assumed not to be depleted significantly. This is a reasonable assumption because the source concentration is insignificantly altered by resuspension, (i.e., resuspension rates are usually small compared to the 3.2×10^{-7} seconds in a year). Because resuspension rates are on the order of 10^{-11} to 10^{-7} fraction resuspended per second, the concentration of the source is nearly independent of time.

To confirm these low resuspension rates, tracer source concentrations were determined at a 29.9-m circular resuspension site near Horn Rapids Dam in the Hanford area (Sehmel 1983b). Although resuspension rates indicate that the $CaMoO_4$ source was depleted very little, source concentrations (amount per unit surface area) showed significant variations from the uniform source concentration originally deposited in the tracer-source area. Also, the source area had increased in size because resuspended tracer had redeposited (mainly tracer that was transported by surface creep and saltation mechanisms).

The objective of this investigation was to evaluate the variations in the concentration of source within the original tracer-source area, and to determine the rate of increase in the size of the source area at a second source site of tracer.

Experiments

The second tracer source is an annular area near the Hanford Meteorological Station tower that is vegetated principally with cheat grass (*Bromus tectorum*). The annular sector was oriented to maximize measured airborne concentrations during high wind speeds. The tracers deposited were calcium molybdate (nearly insoluble) and lithium carbonate (very soluble). On October 3, 1980, the tracers were deposited at concentrations of 19.6 g Mo/m^2 and 0.46 g Li/m^2. Calcium molybdate had been deposited at the site previously (October, 1975) at a concentration of 9.4 g Mo/m^2. Hence, if the source-strength concentration is undepleted from the two tracer deposits, the total molybdenum concentration on the ground should be 29.0 g Mo/m^2.

Soils were sampled during November 1982, two years after both tracers were deposited. Samples were collected at locations shown in Figure 1. To identify the sampling sites the four corners of the annular sector are labelled A, B, C, and D. Edges A-B and C-D are straight, corresponding to wind directions of 190° and 260°, respectively. In contrast, edges B-C and D-A are arcs centered on location O. In addition, the edge distance between corners B and C is approximated by a single arc from B to C, centered at location O. Samples were collected 0.3 m inside the original tracer source area, and at distances of 0.8, 3, and 9 m outside the original tracer source area. Samples were collected from a 84-cm^2 surface area, and at an average soil depth of 1 cm. After soil collection, soil samples were dried, weighed, and leached with 2 M citric acid for dissolving and chelating molybdenum. Leach solutions were analyzed with an induction-coupled argon plasma atomic emission spectrometer (ICP).

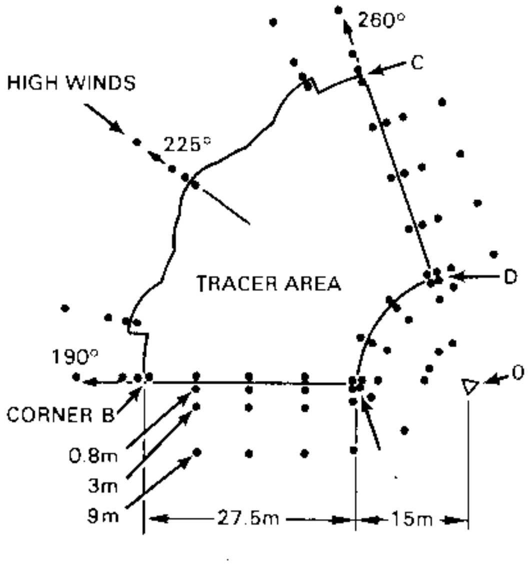

FIGURE 1 Soil Sampling Locations at the Annualar-Sector Tracer-Source Area

Results

Molybdenum and lithium concentrations are shown in Figures 2 and 3, respectively, as a function of distance along the edge of the annular sector. Distances are referenced successively from each corner (i.e., corners A, B, C, and D). For both tracers, average concentrations of source within the original tracer-source area are all less than the total concentration source when originally deposited, and concentrations of source decrease rapidly with distance beyond the original area. Decreases in source concentrations are assumed to reflect background concentrations at 9 m.

Conclusions

Water solubility is an important parameter affecting resuspension source-concentration changes with time. As expected, significant differences in source-concentration were measured for the water soluble and insoluble tracers. For the water soluble tracer (Li_2CO_3), maximum source concentrations in the original tracer area were two orders of magnitude less than when deposited (i.e., 1.5 x 10^{-2} g Li/m^2 after two years weathering from an original source-strength of 0.46 g Li/m^2). For the water insoluble tracer ($CaMoO_4$), the maximum source-strength concentrations in the original tracer area was the same as when deposited (i.e., 35.3 g Mo/m^2 as compared to average of 29.0 g Mo/m^2 deposited).

References

Sehmel, G. A. 1983a. "Resuspension Rates from Aged Inert-Tracer Sources." In Precipitation Scavenging, Dry Deposition, and Resuspension, eds. H. R. Pruppacher, R. G. Semonin, and W. G. N. Slinn, Elsevier, New York, pp. 1073-1086.

Sehmel, G. A. 1983b. "Tracer Resuspension Source-Strength Spread on the Surface by Wind Resuspension." In Pacific Northwest Laboratory Annual Report for 1982 to the DOE Office of Energy Research, Atmospheric Sciences, PNL-4600-3, pp. 33-44, Pacific Northwest Laboratory, Richland, WA.

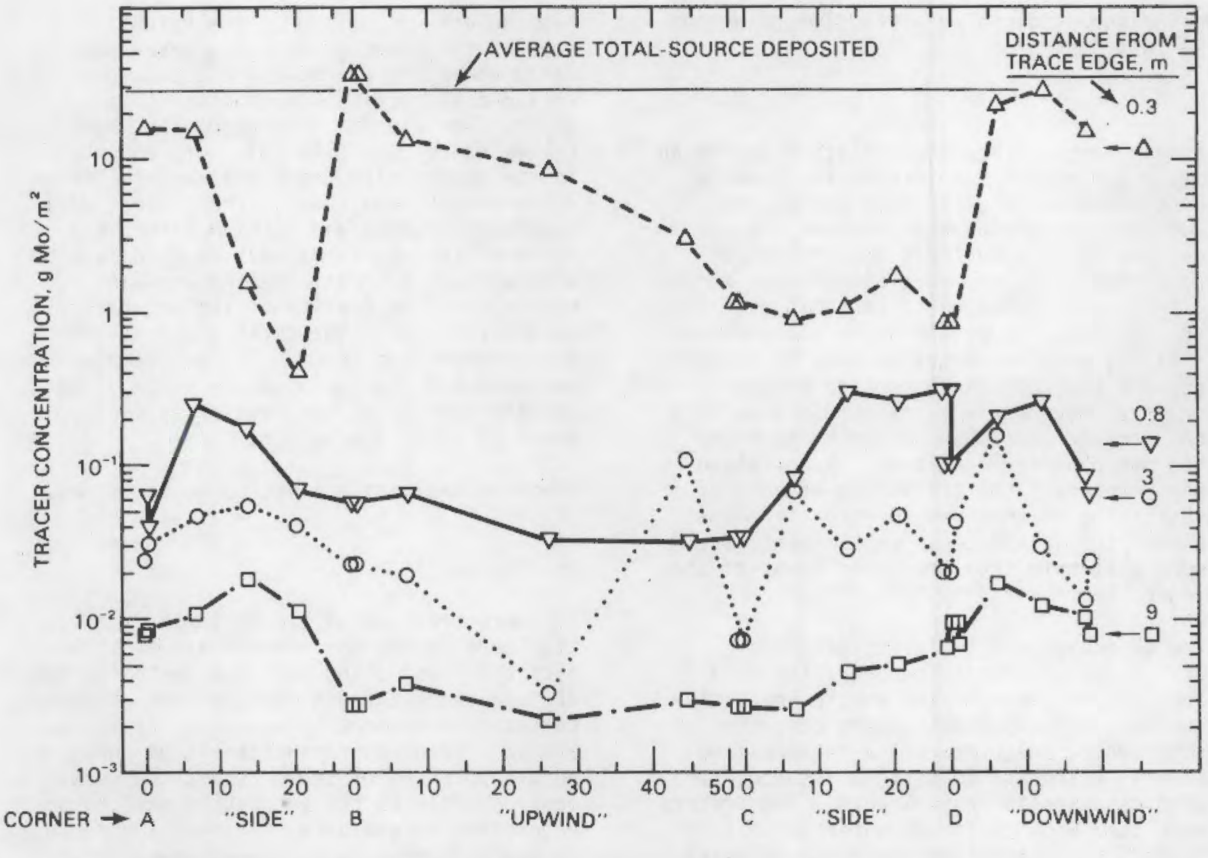

FIGURE 2 Molybdenum-Tracer Source Strength per Square Meter of Ground Surface as a Function of Distance from the Edge of the Original Tracer Source Area

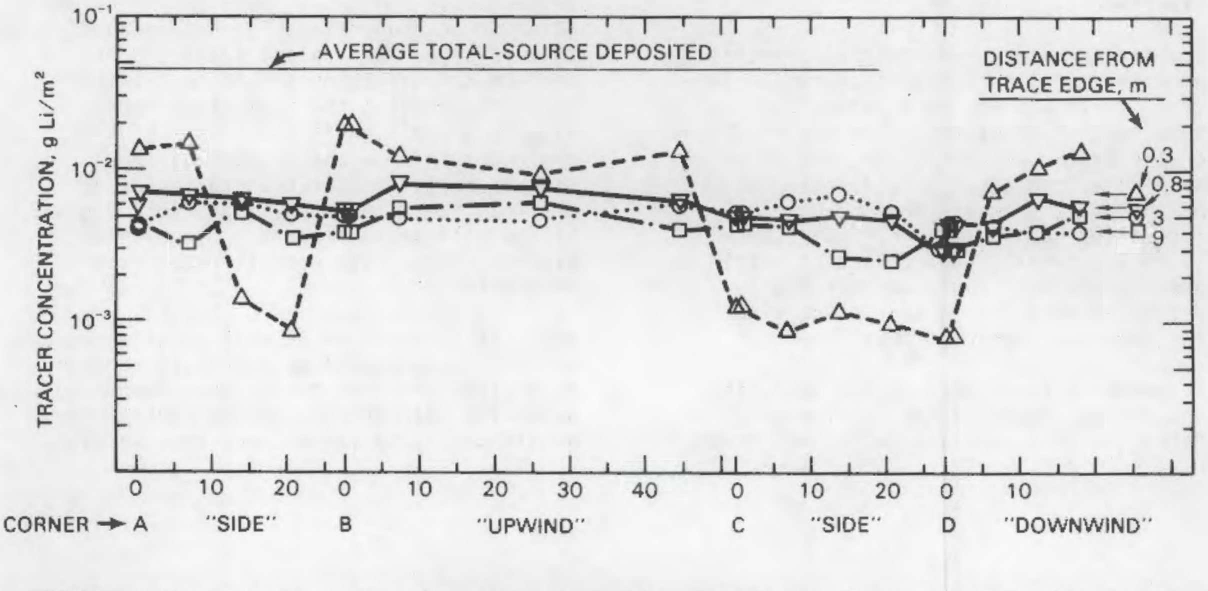

FIGURE 3. Lithium-Tracer Source Strength per Square Meter of Ground Surface as a Function of Distance from the Edge of the Original Tracer Source Area

RESUSPENDED TRACER AS A FUNCTION OF HEIGHT ON CHEAT GRASS

G. A. Sehmel

Resuspended surface contamination may be an important vector for introducing chemical contamination into the food chain. In addition to resuspension by wind, resuspension of radionuclides by rain-splash onto vegetation may be a significant mechanism that contributes to contaminant transport to man. As discussed in the previous article, wind resuspension does not rapidly deplete the contaminant source on the ground. Nevertheless, raindrops impacting the ground may resuspend contaminants to the surrounding vegetation. Rain-splash may counteract the inhibiting effects of vegetation on wind resuspension from the underlying soil because contaminants are more available from the upper layer of the vegetation.

The objective was to investigate distributions of tracer concentration as a function of their height on the vegetative canopy. The experiments were conducted at sites where inert tracers were deposited several years ago to serve as sources for wind-resuspension experiments. Two tracers were used with different water solubilities: calcium molybdate, which is nearly insoluble, and lithium carbonate, which is very soluble.

Experimental Procedures

The tracer sites are vegetated principally with cheat grass (Bromus tectorum). The cheat grass was the only vegetation sampled. To investigate the distributions of the tracer concentration, the grass was sampled at two sites as a function of height above ground. Samples were collected for height increments of 2.5 cm (1 in.). Samples were collected within areas where the tracer was originally deposited as a tracer source for wind resuspension investigations.

At one site (near Horn Rapids Dam), the only tracer released was calcium molybdate. At this site vegetation was removed from an area of 0.11 m^2. The height of some of the cheat grass was greater than 36 cm above the ground. The top sample included all vegetation growing above 36 cm. The average density of the vegetative canopy was 0.14 kg/m^2 dry weight. At the second site (near the Hanford Meteorological Station tower), the tracers were calcium molybdate and lithium carbonate. At this site vegetation was removed from an area of 0.11 m^2. The cheat grass was higher, but the density of the vegetative canopy was less. The cheat grass height was greater than 46 cm. The top sample included all vegetation above 46 cm. The average density of the vegetative canopy was 0.10 kg/m^2 dry weight.

Chemical analyses are yet to be performed.

Conclusions

If concentrations of tracer on the vegetation were large, the results may be significant in evaluating possible contamination of food crops through resuspension of contaminants from underlying soil. If resuspended surface contamination is on the edible portions of cover crops, the resuspension rates to the vegetation need to be determined to evaluate the ingestion route. Currently, these rates are unknown.

Low concentrations on the vegetation may reflect that tracer previously resuspended by rain-splash onto the vegetation was subsequently removed by wind resuspension after vegetation dried. To determine if this is true, rain-splash transport of surface contamination should be investigated by sampling the vegetation immediately after significant rain. If tracer concentrations on the vegetation are significantly greater than those concentrations in the current sample set, vegetation will be sampled as a function of time to investigate removal rates from vegetation.

Rates of rain-splash as well as wind resuspension rates should be evaluated through both field and wind tunnel experiments to determine whether rain-splash contributes significantly to contaminant resuspension.

• Theoretical Studies and Application

Objectives of this study are:

Developing mathematical models to realistically characterize and describe the fate of energy-related air contaminants.

Translating theory and data into forms most useful for practical application in evaluating the consequences of air contaminant releases.

THEORETICAL STUDIES AND APPLICATION

W. G. N. Slinn

This brief report summarizes progress on this project during FY 1983. Some publications resulting from the efforts on this project this year were:

1. The book "Air-Sea Exchange of Gases and Particles," P. S. Liss (U.K.) and W. G. N. Slinn (eds.), Reidel, Holland.
2. The two-volume conference proceedings "Precipitation Scavenging, Dry Deposition, and Resuspension," H. R. Pruppacher (UCLA), R. G. Semonin (ISWS), and W. G. N. Slinn (coords.), Elsevier, New York.
3. The two papers "A Potpourri of Deposition and Resuspension Questions," by W. G. N. Slinn and "Inland Transport, Mixing, and Dry Deposition of Sea-Salt Particles," by P. C. Katen (OSU), L. F. Radke (U of W), and W. G. N. Slinn, which were presented at the "Chamberlain Conference" and contained in the Proceedings.
4. A paper, coauthored with T. W. Horst, concerned with airborne-pesticide profiles above treated fields and with the development of some general theory about resuspension and vertical mixing. A summary of this paper is given elsewhere in this annual report.

The "Chamberlain Conference"

FY 1983 saw the culmination of substantial effort by the principal investigator (P.I.), in cochairing the Fourth International Conference on Precipitation Scavenging, Dry Deposition, in Santa Monica, California during November 29 through December 3, 1982. The honorary chairman of the meeting was Dr. A. C. Chamberlain, AERE Harwell; the other cochairmen were H. R. Pruppacher and R. G. Semonin; members of the Steering Committee were P. Buat-Menard, J. A. Garland, D. F. Gatz, H. W. Georgii, D. A. Gillette, B. B. Hicks, H. Rodhe, G. A. Sehmel, P. W. Summers, and O. Vittori. Approximately 250 people attended, and approximately 125 papers were presented. The Proceedings have already been published as the two-volume hard-cover set "Precipitation Scavenging, Dry Deposition, and Resuspension" by Elsevier. Via this conference, the quality of science in these fields was improved.

Some Scientific Contributions

In the reports listed in the Introduction more complete descriptions are given of the following scientific advances made by the P.I.

- Via regular perturbation methods, it was shown that for Stokes number smaller than the critical value, particle inertia can decrease interception's contribution to the collision efficiency between an aerosol particle and an obstacle.
- Additional analyses were presented, demonstrating that with present instrument capabilities, it is essentially impossible (because of time variations and inhomogenieties) to use eddy-flux or gradient methods to perform atmospheric measurements of the air/surface exchange of substances if their net exchange rate is less than about 0.1 cm/sec.
- By extending the P.I.'s published models for precipitation scavenging and dry deposition, new predictions were made for the contribution of spray to the "dry" deposition of particles to lakes and other water bodies.

- By comparing the magnitudes of the fluxes, theoretical justification was developed for the use of Henry's law in nonequilibrium conditions.

- A simple derivation of the Rayleigh instability criterion was developed, based on thoe proposal that convection is inhibited if heat transfer by conduction is faster than by convection, and applied to the problem of interfacial mass transfer for conditions of convective instabilities.

- A new model was developed for the aerodynamic roughness of water bodies. This model relies on the assumption that at least part of the roughness is proportional to the height of induced capillary waves. Consequently, the resulting roughness contains the influence of surface tension (in contrast to the Charnock relation).

- It was demonstrated that previous studies, reportedly of the particle-size independence of the dry deposition of sea-salt particles, were likely misinterpretations caused by ignoring the influence of changing meteorological conditions.

- A theoretical basis was developed for the integral-equation approach to describing air-surface exchange plus atmospheric diffusion; this result is outlined elsewhere in this report.

Other Activities

Three other activities also absorbed substantial time during this year. The book (published this year) entitled "Air-Sea Exchange of Gases and Particles" was edited and the report by the National Academy of Sciences dealing with acidic deposition in eastern North America was reviewed. The P.I. also helped in designing new DOE initiatives in precipiation scavenging, in dry deposition, and in modeling the long-range transport of air pollution.

Publications and Presentations

PUBLICATIONS

Doran, J. C. and T. W. Horst. 1983. "Observations and Models of Simple Nocturnal Slope Flows." *J. Atmos. Sci.* 40:708-717.

Horst, T. W. 1983. "A Correction to the Gaussian Source Depletion Model." In: *Precipitation Scavenging, Dry Deposition and Resuspension*, eds. H. R. Pruppacher, R. G. Semonin, and W. G. N. Slinn. Elsevier Science Publishing Co., Amsterdam, The Netherlands.

Horst, T. W. and J. C. Doran. 1983. "Nocturnal Drainage Flow on Simple Slopes: An ASCOT Progress Report." PNL-SA-11245, Pacific Northwest Laboratory, Richland, Washington.

Horst, T. W. and W. G. N. Slinn. 1983. "Atmospheric Concentrations of Pesticides Above Treated Fields." Submitted for publication in *Science*.

Horst, T. W. and W. G. N. Slinn. 1983. "Estimates for Pollution Profiles Above Finite Area-Sources." Submitted for publication in *Atmospheric Environment*.

Liss, P. S. and W. G. N. Slinn (eds.). 1983. *Air-Sea Exchange of Gases and Particles*. In *Proceedings of the NATO Advanced Study Institute on Air-Sea Exchange of Gases and Particles*, University of New Hampshire, Durham, New Hampshire, July 19-30, 1982. *NATO ASI Series, Series C, Mathematical and Physical Sciences No. 108*, D. Reidel Publishing Co., Dordrecht/Boston/Lancaster.

Orgill, M. M. and J. M. Thorp. 1983. "Energy and Air Quality." *EOS Transactions, American Geophysical Union*. *64(41)*:585 and 587.

Orgill, M. M., R. N. Lee and R. I. Schreck. 1983. *Transport of Tracers and Pollutants from The Geysers Geothermal Resource Area.* PNL-4797, Pacific Northwest Laboratory, Richland, Washington.

Pruppacher, H. R., R. G. Semonin, and W. G. N. Slinn (eds.). 1983. "Precipitation Scavenging, Dry Deposition, and Resuspension." Vol. 1: *Precipitation Scavenging*; Vol. 2: *Dry Deposition and Resuspension.* In *Proceedings of the Fourth International Conference (the Chamberlain Conference) on Precipitation Scavenging, Dry Deposition, and Resuspension*, Santa Monica, California, November 29-December 3, 1982. Elsevier Science Publishing Co., Inc., New York/Amsterdam/Oxford.

Sehmel, G. A. 1983. "A Relationship Between Plutonium Activity Densities on Airborne and Surface Soils." PNL-SA-9563, *Health Physics J.* In press.

Sehmel, G. A. 1983. "Particle Dry Deposition Investigated with Tracer Concentration Ratios as a Function of Height." *Aerosol Science and Tech.* 2(2):261.

Sehmel, G. A. 1983. "Particle Dry Deposition Measurements with Dual Tracers in Field Experiments." In *Precipitation Scavenging, Dry Deposition, and Resuspension*, eds. H. R. Pruppacher, R. G. Semonin, and W. G. N. Slinn. Elsevier Science Publishing Co., New York, pp. 1013-1025.

Sehmel, G. A. 1983. "Resuspension Rates from Aged Inert-Tracer Sources." In *Precipitation Scavenging, Dry Deposition, and Resuspension*, eds. H. R. Pruppacher, R. G. Semonin, and W. G. N. Slinn. Elsevier Science Publishing Co., New York, pp. 1073-1086.

Sehmel, G. A. 1983. "Characteristics of Airborne Plutonium Resuspended from Near-Background Aged Surface-Sources." In *Precipitation Scavenging, Dry Deposition, and Resuspension*, eds. H. R. Pruppacher, R. G. Semonin, and W. G. N. Slinn. Elsevier Science Publishing Co., New York, pp. 1145-1159.

Sehmel, G. A. 1983. "Resuspension and Dry Deposition Research Needs." In *Precipitation Scavenging, Dry Deposition, and Resuspension*, eds. H. R. Pruppacher, R. G. Semonin, and W. G. N. Slinn. Elsevier Science Publishing Co., New York, pp. 1435-1441.

Slinn, W. G. N. 1983a. "A Potpourri of Deposition and Resuspension Questions." In *Precipitation Scavenging, Dry Deposition, and Resuspension*, eds. H. R. Pruppacher, R. G. Semonin, and W. G. N. Slinn. Elsevier Science Publishing Co., New York, pp. 1361-1416.

Slinn, W. G. N. 1983b. "Sources and Surface-Area Distributions of Atmospheric Particles." *Atmos. Environ.* 17:2363-2364.

Slinn, W. G. N. 1983c. "Air-to-Sea Transfer of Particles." Chapter 7 of *Air-*

Sea Exchange of Gases and Particles, eds. P. S. Liss and W. G. N. Slinn. D. Reidel Publishing Co., Boston.

Slinn, W. G. N. 1983d. "Precipitation Scavenging." Chapter 11 of Atmospheric Sciences and Power Production, ed. D. Randerson. Available from the U.S. Department of Energy Technical Information Center, Oak Ridge, Tennessee.

Slinn, W. G. N., L. F. Radke and P. C. Katen. 1983. "Inland Transport, Mixing, and Dry Deposition of Sea-Salt Particles." In Precipitation Scavenging, Dry Deposition, and Resuspension, eds. H. R. Pruppacher, R. G. Semonin, and W. G. N. Slinn. Elsevier Science Publishing Co., New York, pp. 1037-1046.

PRESENTATIONS

Doran, J. C. and T. W. Horst. 1983. "Observations of Drainage Winds on a Simple Slope." Paper presented at the Sixth AMS Symposium on Turbulence and Diffusion, Boston, Massachusetts. Published by the American Meteorological Society, Boston, Massachusetts.

Horst, T. W. 1982. "A Correction to the Gaussian Source Depletion Model." Paper presented at the Fourth Conference on Precipitation Scavenging, Dry Deposition and Resuspension, Santa Monica, California. Published by Elsevier Science Publishing Co., Amsterdam, The Netherlands.

Kalwarf, D. R. 1983. "Ozonation Kinetics of Polycyclic Aromatic Nitro Compounds." Paper presented at the National Meeting of the American Chemical Society, August 28-September 2, 1983, Washington, D.C.

Orgill, M. M., R. N. Lee, P. W. Nickola and R. I. Schreck. 1983. "Hydrogen Sulfide, Trace Element and Sulfur Hexafluoride Tracer Transport from The Geysers-Calistoga Geothermal Resource Area Based on Aircraft and Surface Sampling." In Proceedings of the Sixth Symposium on Turbulence and Diffusion, American Meteorological Society, March 22-25, 1983, Boston, Massachusetts, pp. 192-195.

Sehmel, G. A. 1983. "Particle Dry Deposition Investigated with Tracer Concentration Ratios as a Function of Height." PNL-SA-10965. Paper presented at the American Association of Aerosol Research Annual Meeting, April 18-22, 1983, College Park, Maryland.

Sehmel, G. A. 1983. "Transuranic Resuspension." PNL-SA-11792. Paper presented at the Department of Energy Symposium on Environmental Research for Actinide Elements, November 7-11, 1983, Hilton Head Island, South Carolina.

Slinn, W. G. N. 1982a. "Inland Transport, Mixing, and Dry Deposition of Sea-Salt Particles." Paper presented at the Fourth International Conference on Precipitation Scavenging, Dry Deposition, and Resuspension, November 29-December 3, 1982, Santa Monica, California.

Slinn, W. G. N. 1982b. "A Potpourri of Deposition and Resuspension Questions." Paper presented at the Fourth International Conference on Precipitation Scavenging, Dry Deposition, and Resuspension, November 29-December 3, 1982, Santa Monica, California.

Author Index

AUTHOR INDEX

Organization Charts
Distribution

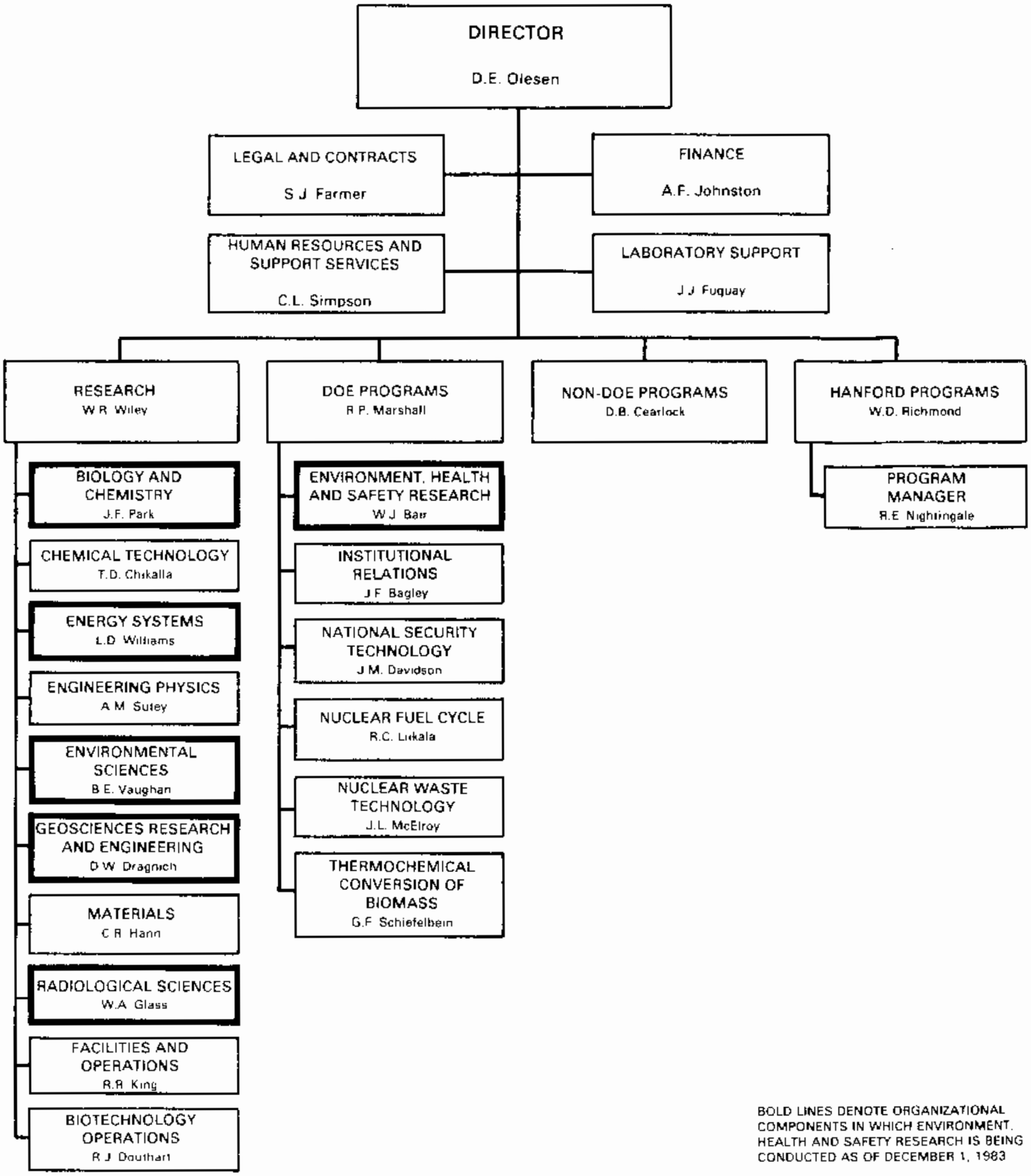

BOLD LINES DENOTE ORGANIZATIONAL COMPONENTS IN WHICH ENVIRONMENT, HEALTH AND SAFETY RESEARCH IS BEING CONDUCTED AS OF DECEMBER 1, 1983

ENVIRONMENT, HEALTH AND SAFETY RESEARCH

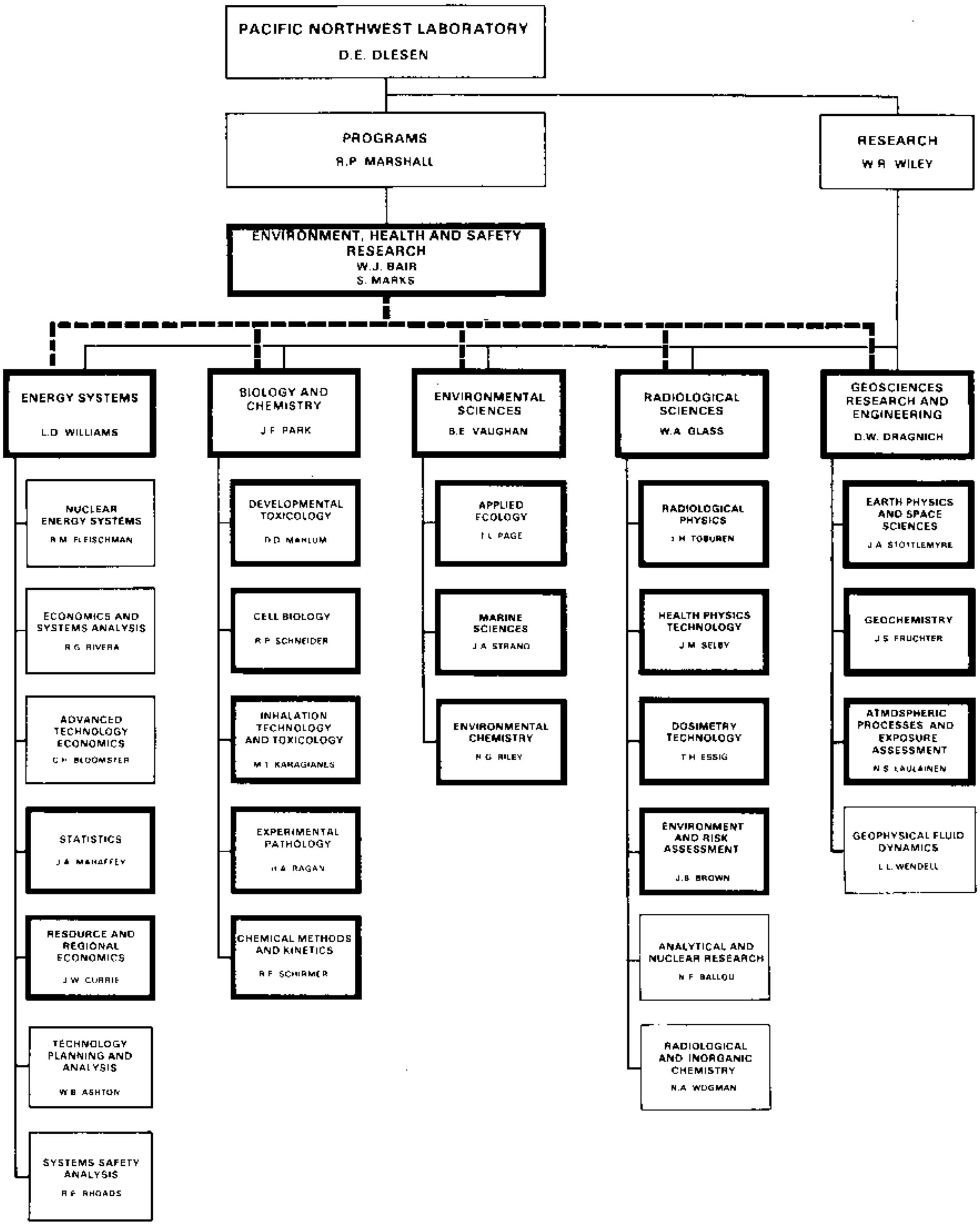

NOTE

▬ BOLD LINES DENOTE ORGANIZATIONAL COMPONENTS IN WHICH HEALTH AND ENVIRONMENTAL RESEARCH IS BEING CONDUCTED AS OF DECEMBER 1, 1983

— FUNCTIONAL MANAGEMENT RELATIONSHIP

▬ ▬ ▬ EH&SR PROGRAM MANAGEMENT RELATIONSHIP

DISTRIBUTION

PNL-5000 PT-3
UC-11

No. of
Copies

OFFSITE

27 DOE Technical Information
Center

W. P. Albers
Environmental Protection
Safety and Emergency
Preparedness
U.S. Department of Energy
Washington, DC 20545

R. Alexander
Nuclear Regulatory
Commission
Washington, DC 20545

E. L. Alpen
Lawrence Berkeley
Laboratory
University of California
Building 90, Room 2056
No. 1 Cyclotron Road
Berkeley, CA 94720

J. A. Auxier
Oak Ridge National
Laboratory
P.O. Box X
Oak Ridge, TN 37830

J. S. Ball
Bartlesville Energy
Research Center
U.S. Department of Energy
P.O. Box 1398
Bartlesville, OK 74003

D. Ballantine
Office of Energy Research
U.S. Department of Energy
Washington, DC 20545

R. Barber
Office of Environmental
Protection Safety &
Emergency Preparedness
U.S. Department of Energy
Washington, DC 20545

N. F. Barr
Office of Energy Research
U.S. Department of Energy
Washington, DC 20545

No. of
Copies

E. W. Bean
Rocky Flats Area Office
DOE - Albuquerque
Operations Office
P.O. Box 928
Golden, CO 80401

J. A. Bibb
DOE - Oak Ridge
Operations Office
P.O. Box E
Oak Ridge, TN 37830

J. Birely
Los Alamos Scientific
Laboratory
University of California
P.O. Box 1663
Los Alamos, NM 87545

V. P. Bond
Brookhaven National
Laboratory
Upton, Long Island,
NY 11973

L. C. Brazely, Jr.
Office of Operational
Protection, Safety &
Emergency Preparedness
U.S. Department of Energy
EP-32, GTN
Germantown, MD 20545

L. Bustad, Dean
College of Veterinary
Medicine
Washington State
University
Pullman, WA 99163

J. Coleman
Office of Energy Research
U.S. Department of Energy
Washington, DC 20545

Council of Environmental
Quality
72 Jackson Place, N.W.
Washington, DC 20006

R. W. Davies
Office of Environmental
Protection Safety &
Emergency Preparedness
U.S. Department of Energy
Washington, DC 20545

No. of
Copies

J. J. Davis
Asst. Director of
Research
Nuclear Regulatory
Commission
Washington, DC 20545

A. W. Decora
Laramie Energy Research
Center
U.S. Department of Energy
P.O. Box 3395
Laramie, WY 83071

H. Drucker
Argonne National
Laboratory
Argonne, IL 60439

A. P. Duhamel
Office of Energy Research
U.S. Department of Energy
Washington, DC 20545

P. B. Dunnaway
DOE - Oak Ridge
Operations Office
P.O. Box 14100
Las Vegas, NV 89114

C. W. Edington
Office of Energy Research
U.S. Department of Energy
Washington, DC 20545

H. Ellett
Environmental Protection
Agency
Washington, DC 20460

B. M. Erickson
DOE - Schenectady Naval
Reactors Office
P.O. Box 1069
Schenectady, NY 12301

G. H. Gronhovd
Grand Forks Energy
Research Center
U.S. Department of Energy
P.O. Box 8213
Grand Forks, ND 58202

E. Harvey
Office of Energy Research
U.S. Department of Energy
Washington, DC 20545

No. of
Copies

J. W. Healy
Los Alamos Scientific
Laboratory
University of California
P.O. Box 1663
Los Alamos, NM 87545

H. L. Hollister
Office of Environmental
Protection Safety &
Emergency Preparedness
U.S. Department of Energy
Washington, DC 20545

C. Jackson
DOE - San Francisco
Operations Office
133 Broadway
Wells Fargo Building
Oakland, CA 94616

J. F. Johnson
Kenworth Truck Co.
30 Vreeland Road
Florham Park, NJ 07932

L. J. Johnson
EG&G Idaho
Box 1625
Idaho Falls, ID 83415

G. Y. Jordy, Director
Office of Program
Analysis
Office of Energy Research
U.S. Department of Energy
ER-30, GTN
Germantown, MD 20545

J. Kane
Office of Energy Research
U.S. Department of Energy
Washington, DC 20545

F. Koomonoff
Office of Energy Research
U.S. Department of Energy
Washington, DC 20545

Library
Bartlesville Energy
Research Center
U.S. Department of Energy
P.O. Box 1398
Bartlesville, OK 74005

Librarian
Joint Center for Graduate
Study
100 Sprout Road
Richland, WA 99352

No. of
Copies

Librarian
Lawrence Livermore
Laboratory
University of California
Technical Information
Department, L-3
P.O. Box 808
Livermore, CA 94500

Librarian
Los Alamos Scientific
Laboratory
P.O. Box 1663
Los Alamos, NM 87545

Reference Librarian
Research Library
Brookhaven National
Laboratory
Upton, Long Island,
NY 11973

W. J. Little, Jr.
Office of Environmental
Protection Safety &
Emergency Preparedness
U.S. Department of Energy
Washington, DC 20545

J. N. Maddox
Office of Energy Research
U.S. Department of Energy
Washington, DC 20545

J. R. Maher
Acting Director
Office of Nuclear Safety
Environmental Protection,
Safety and Emergency
Preparedness
U.S. Department of Energy
EP-34, GTN
Germantown, MD 20545

C. R. Mandelbaum
Office of Program
Analysis
Office of Energy Research
U.S. Department of Energy
ER-32, GTN
Germantown, MD 20545

D. D. Mayhew
Office of Energy Research
U.S. Department of Energy
Washington, DC 20545

H. McCammon
Office of Energy Research
U.S. Department of Energy
Washington, DC 20545

No. of
Copies

J. W. McCaslin
INEL, Aerojet Nuclear
550 Second Street
Idaho Falls, ID 83401

R. O. McClellan
Inhalation Toxicology
Research Institute
Lovelace Foundation for
Medical Education and
Research
P.O. Box 5890
Albuquerque, NM 87115

T. F. McCraw
Office of Environmental
Protection Safety &
Emergency Preparedness
U.S. Department of Energy
Washington, DC 20545

C. B. Meinhold
Brookhaven National
Laboratory
Upton, Long Island,
NY 11973

M. L. Mendelsohn
Lawrence Livermore
Laboratory
University of California
P.O. Box 808
Livermore, CA 94550

M. L. Minthorn, Jr.
Office of Energy Research
U.S. Department of Energy
Washington, DC 20545

B. Morgan
DOE - Savannah River
Operations Office
P.O. Box A
Aiken, SC 29801

W. E. Mott
Office of Operational
Safety
Environmental Protection,
Safety andd Emergency
Preparedness
U.S. Department of Energy
EP-323, GTN
Germantown, MD 20545

No. of
Copies

W. R. Ney
Executive Director
National Council on
Radiation Protection
and Measurement
7910 Woodmont Avenue
Suite 1061
Washington, DC 20014

NRC Advisory Committee
on Reactor Safeguards
Washington, DC 20555

D. E. Patterson
Environmental Protection
Safety and Emergency
Preparedness
U.S. Department of Energy
Washington, DC 20545

A. A. Pitrolo
Morgantown Energy
Research Center
U.S. Department of Energy
P.O. Box 880
Morgantown, WY 26505

R. G. Rader
Office of Energy Research
U.S. Department of Energy
ER-32, GTN
Germantown, MD 20545

D. Rall, Director
National Institute of
Environmental Health
Standards
P.O. Box 12233
Research Triangle Park,
NC 27709

R. Ray
DOE - Nevada Operations
Office
P.O. Box 14100
Las Vegas, NV 89114

W. Reese
DOE - Savannah River
Operations Office
P.O. Box A
Aiken, SC 29801

C. R. Richmond
Oak Ridge National
Laboratory
P.O. Box X
Oak Ridge, TN 37830

No. of
Copies

J. R. Roeder
DOE - Albuquerque
Operations Office
P.O. Box 5400
Albuquerque, NM 87115

R. A. Scarano
Nuclear Regulatory
Commission
Mill Licensing Section
Washington, DC 20545

M. Schulman
Office of Energy Research
U.S. Department of Energy
Washington, DC 20545

D. H. Slade
Office of Energy Research
U.S. Department of Energy
Washington, DC 20545

J. Snow
Office of Energy Research
U.S. Department of Energy
ER-6, FORR
Washington, DC 20585

J. H. Spickard
DOE - Idaho Operations
Office
550 Second Street
Idaho Falls, ID 83401

J. F. Stevens
Dayton Area Office
U.S. Department of Energy
P.O. Box 66
Miamisburg, OH 45342

Frank Swanberg
Nuclear Regulatory
Laboratory
Washington, DC 20545

J. Swinebroad
Office of Environmental
Protection Safety &
Emergency Preparedness
U.S. Department of Energy
Washington, DC 20545

Technical Information
Service
Room 773A
Savannah River Laboratory
E. I. du Pont de Nemours
and Company
Aiken, SC 29801

No. of
Copies

J. W. Thiessen
Office of Energy Research
U.S. Department of Energy
Washington, DC 20545

A. Trivelpiece
Office of Energy Research
U.S. Department of Energy
Washington, DC 20545

W. Vaughan
Office of Environmental
Protection Safety &
Emergency Preparedness
U.S. Department of Energy
Washington, DC 20545

G. L. Voelz
University of California
Los Alamos Scientific
Laboratory
P.O. Box 1663
Los Alamos, NM 87545

H. L. Volchok
Environmental Measurements Laboratory
376 Hudson Street
New York, NY 10014

B. W. Wachcholz
Low Level Radiation
Branch
National Institute
of Health
Landon Bldg/Rm 8C-09
9000 Rockville Pike
Bethesda, MD 20205

I. Wender
Pittsburgh Energy
Research Center
4800 Forbes Avenue
Pittsburgh, PA 15213

W. Weyzen
Electric Power Research
Institute
3412 Hillview Avenue
Palo Alto, CA 92665

M. M. Williamson
DOE - Idaho Operations
Commission
550 Second Street
Idaho Falls, ID 83401

R. W. Wood
Office of Energy Research
U.S. Department of Energy
Washington, DC 20545

No. of
Copies

R. E. Yoder
Rockwell International
P.O. Box 464
Golden, CO 80401

Zhu Zhixian
Laboratory for Energy-
Related Health Research
University of California
Davis, CA 96616

FOREIGN

M. Anderson
Library
Department of National
Health and Welfare
Ottawa, Ontario
CANADA

J. K. Basson
Vice-President
Raad Op Atomic
Atoomkrag Energy Board
Privaatsk X 256
Pretoria 0001
REPUBLIC OF SOUTH AFRICA

Z. M. Beekman
President of IRPA
Rooseveltlaan 197
1079 AP Amsterdam
THE NETHERLANDS

A. Brink
Sasol-One Limited
P.O. Box 1
Sasolburg 9570
REPUBLIC OF SOUTH AFRICA

Niels Busch
Director, Risø National
Laboratory
DK-40000 Roskilde
DENMARK

G. H. Clark
Australian Atomic Energy
Commission
Private Mail Bag
Sutherland NSW 2232
AUSTRALIA

No. of
Copies

H. Daw
Director, Division of
Health, Safety and
Waste Management
International Atomic
Energy Agency
Vienna 1,
Kaerntnerring 11
AUSTRIA

Li De-ping
Professor and Director
of North China
Institute of Radiation
Protection, MNI
Tai-yuan, Shan-xi
THE PEOPLE'S REPUBLIC
OF CHINA

Director
Commissariat a l'Energie
Atomique
Centre d'Etudes
Nucléaires de
Fontenay-aux-
Roses (Seine)
FRANCE

Director
Commonwealth Scientific
and Industrial Research
Organization
Aspendale
Victoria 3195
AUSTRALIA

D. Djuric
Institute of Occupational
Radiological Health
11000 Beograd
Deligradska 29
YUGOSLAVIA

J. Dunster
National Radiological
Protection Board
Harwell, Didcot
Oxfordshire OXII ORQ
ENGLAND

I. Peinendegen
Institut für Medizin
Kernforchung sanlege
Jülich
Postfach 1913
517, Jülicn
FEDERAL REPUBLIC OF
GERMANY

No. of
Copies

A. R. Gopal-Ayengar
Institut fur Biophysik
Herrenhauser Str. 2
3000 Hannover, 21
FEDERAL REPUBLIC OF
GERMANY

Wang Hengde
North China Institute of
Radiation Protection
P.O. Box 120
Taiyuan City, Shanxi
Province
THE PROPLE'S REPUBLIC
OF CHINA

W. Jacobi
Institut fur
Strahlenschutz
D-8042 Neuherberg
Ingolstaddter
Landstrasse 1
FEDERAL REPUBLIC OF
GERMANY

K. E. Lennart Johansson
National Defense Research
Institute
FOA 45 1 S-901-82
Umea, SWEDEN

H. J. Klimisch
BASF Aktiengesellschaft
Abteilung Toxikologie
6700 Ludwishafen
FEDERAL REPUBLIC OF
GERMANY

Lief Kristensen
Physics and Meteorology
Risø National Laboratory
DK-4000 Roskilde
DENMARK

E. Komarov
Environmental Health
Division
World Health Organization
Avenue Appia 1211
Geneva 27, SWITZERLAND

T. Kumatori
Director
National Institute of
Radiological Sciences
4-9-1, Anagawa
Chiba-shi, Chiba 260
JAPAN

No. of
Copies

Professor D. Lal
Physical Research
Laboratory
Ahmedabad
380 009
INDIA

Librarian
Australian AEC
Private Mail Bag
Sutherland
NSW 2232
AUSTRALIA

Librarian, Building 465
Atomic Energy Research
Establishment
Harwell, Didcot
OXON OXII ORD
ENGLAND

Librarian
Centre d'Etudes
Nucleaires de Saclay
P.O. Box 2, Saclay
Fig-sur-Yvette (S&O)
FRANCE

Librarian
Commonwealth Scientific
and Industrial Research
Organization
314 Albert Street
P.O. Box 89
East Melbourne, Victoria
AUSTRALIA

Shu-Zheng Liu, M.D.
Department of Radiation
Biology
Bethune Mediacal
University
7 Xinmin Street
Changchun, Jilin
THE PEOPLE'S REPUBLIC
OF CHINA

Wei Luxin
Laboratory of Industrial
Hygiene
Ministry of Public
Health
2 Xinkang Street
Deschengmenwai, Beijing
THE PEOPLE'S REPUBLIC
OF CHINA

No.of
Copies

A. M. Marko
Director Atomic Energy
of Canada Ltd.
Biology and Health
Physics Division
Chalk River Nuclear
Laboratories
Chalk River
Ontario KOJ IJO
CANADA

J. C. Nenot
Comite de Radioprotection
69, Rue de Micromesnil
75008 Paris
FRANCE

B. Otter
Director
Norwegian Institute for
Air Research
Elvegaten 52
N-2000 Lillestrøm
NORWAY

Lars Prahm
National Agency
of Environmental
Protection
Risø National Laboratory
DK-4000 Roskilde
DENMARK

Dr. Vittorio Prodi
Department of Physics
University of Bologna
Via Irnerio 46
40126 Bologna
ITALY

H. Rodhe
Meteorological Institute
Stockholm University
S-10691 Stockholm
SWEDEN

Wang Ruifa
Associate Director
Laboratory of Industrial
Hygiene
Ministry of Public Health
2 Xinkang Street
Deshangmanwai, Beijing
THE PEOPLE'S REPUBLIC
OF CHINA

No. of
Copies

M. Rzekiecki
Commissariat a l'Energie
Atomique
Centre d'Etudes
Nucleaires de Cadarache
BP n 13-St. Paul
Les Durance
FRANCE

Sun Shi-quan
Head of Radiation-
Medicine Department
North China Institute of
Radiation Protection
Tai-Yuan, Shan-xi
THEE PEOPLE'S REPUBLIC
OF CHINA

Cao Shu-yuan
Deputy Head of Laboratory
of Radiation Medicine
North China Institute of
Radiation Protection,
MNI
Tai-Yuan, Shan-xi
THE PEOPLE'S REPUBLIC
OF CHINA

Ruth Skarin, Chief
Librarian
Department of Meteorology
University of Stockholm
Arrhenius Laboratory
S106 91 Stockholm
SWEDEN

H. Smith, Head
Biology Department
National Radiological
Protection Board
Chilton, Didcot
Oxfordshire OXII ORQ
ENGLAND

F. D. Sowby
International Commission
on Radiological
Protection
Clifton Avenue
Sutton, Surrey
ENGLAND

M. J. Suess
Regional Officer for
Environmental Hazards
World Health Organization
8 Scherfigsvej DK-2100
Copenhagen, DENMARK

No. of
Copies

Yibing Wang
North China Institute of
Radiation Protection
P.O. Box 120
Taiyuan City,
Shanxi Province
THE PEOPLE'S REPUBLIC
OF CHINA

B. C. Winkler
Director, Licensing
(Standards)
Raad Op Atoomlrag/Atomic
Energy Board
Privaatsak X 256/
Private Bag X 256
Pretoria 001
REPUBLIC OF SOUTH AFRICA

Chen Xing-an
Laboratory of Industrial
Hygiene
Ministry of Public Health
2 Xinkang Street
Deshengmenwai, Beijing,
THE PEOPLE'S REPUBLIC
OF CHINA

Deng Zhickeng
NorthChina Institute of
Radiation Protection
Taiyuan, Shanxi Province
THE PEOPLE'S REPUBLIC
OF CHINA

ONSITE

2 DOE Richland Operations Office

P. F. X. Dunigan
H. E. Ransom/P. K. Clark

2 Hanford Environmental Health Foundation

D. R. Breitenstein
R. D. Gilmore

Rockwell Hanford Operations

P. G. Lorenzini

No. of
Copies

UNC Nuclear Industries

T. E. Dabrowski

2 Westinghouse Hanford Company

R. O. Budd
D. E. Simpson

8 Battelle-Seattle

S. M. Nealey
E. B. Perrin
J. E. Rasmussen
A. H. Schilling
C. R. Schuller
R. Shikiar
M. E. Walsh
M. T. Wood

6 Battelle Memorial Institute

N. E. Carter
L. L. German
R. S. Paul
D. B. Shipler
C. R. Vest
Librarian

3 Battelle-Columbus

A. H. Adelman
A. D. Barker
F. J. Milford

3 Battelle-Washington DC Office

G. Johnson
S. Stryker
C. Vest

193 Pacific Northwest Laboratory

O. B. Abbey
R. W. Baalman (5)
W. J. Bair (15)
K. M. Busness
T. P. Chikalla

No. of
Copies

M. T. Dana
J. M. Davidson
J. C. Doran
J. L. Downs-Berg
C. E. Elderkin (40)
W. A. Glass
D. W. Glover
R. H. Gray
R. K. Hadlock (5)
J. M. Hales (5)
C. R. Hann
R. V. Hannigan
D. J. Hoitink
T. W. Horst
D. R. Kalkwarf
N. S. Laulainen (50)
R. N. Lee
R. C. Liikala
F. D. Lloyd
S. Marks
R. P. Marshall
J. E. Mendel
J. E. Minor
J. M. Nielson
R. E. Nightingale
D. E. Olesen
M. M. Orgill
W. T. Pennell
A. M. Platt
P. M. Potter (5)
W. D. Richmond
G. F. Schiefelbein
L. C. Schmid
R. I. Schreck
J. B. Schuette
G. A. Sehmel
C. L. Simpson
W. G. N. Slinn
M. E. Stifter
G. M. Stokes
R. A. Stokes (10)
A. M. Sutey
J. M. Thorp
B. E. Vaughan
L. L. Wendell (5)
W. R. Wiley
L. D. Williams
R. K. Woodruff
Biology Library (2)
Technical Information (5)
Publishing Coordination (2)